Positive selection and relaxed purifying selection contribute to rapid evolution of male-biased genes in a dioecious flowering plant

Lei Zhao[1#], Wei Zhou[1#], Jun He[1], De-Zhu Li[1, 2*], Hong-Tao Li[1, 2*]

[1]Germplasm Bank of Wild Species, Yunnan Key Laboratory of Crop Wild Relatives Omics, Kunming Institute of Botany, Chinese Academy of Sciences, Kunming, Yunnan 650201, China

[2]Kunming College of Life Science, University of Chinese Academy of Sciences, Kunming, Yunnan 650201, China

[#] These authors contributed equally to this article

Running title: Positive selection and relaxed selection driving rapid evolution of male-biased genes

*** Corresponding authors:**

Hong-Tao Li lihongtao@mail.kib.ac.cn;

De-Zhu Li dzl@mail.kib.ac.cn

Abstract

Sex-biased genes offer insights into the evolution of sexual dimorphism. Sex-biased genes, especially those with male bias, show elevated evolutionary rates of protein sequences driven by positive selection and relaxed purifying selection in animals. Although rapid sequence evolution of sex-biased genes and evolutionary forces have been investigated in animals and brown algae, less is known about evolutionary forces in dioecious angiosperms. In this study, we separately compared the expression of sex-biased genes between female and male floral buds and between female and male flowers at anthesis in dioecious *Trichosanthes pilosa* (Cucurbitaceae). In floral buds, sex-biased gene expression was pervasive, and had significantly different roles in sexual dimorphism such as physiology. We observed higher rates of sequence evolution for male-biased genes in floral buds compared to female-biased and unbiased genes. Male-biased genes under positive selection were mainly associated with functions to abiotic stress and immune responses, suggesting that high evolutionary rates are driven by adaptive evolution. Additionally, relaxed purifying selection may contribute to accelerated evolution in male-biased genes generated by gene duplication. Our findings, for the first time in angiosperms, suggest evident rapid evolution of male-biased genes, advance our understanding of the patterns and forces driving the evolution of sexual dimorphism in dioecious plants.

Key words: *Trichosanthes pilosa*, positive selection, relaxed purifying selection, sexual dimorphism, sex-biased genes, floral development stages

Introduction

Sexual dimorphism is the condition where sexes of the same species exhibit different morphological, ecological and physiological traits in gonochoristic animals and dioecious plants, despite male and female individuals sharing the same genome except for sex chromosomes or sex-determining loci (Mank, 2009; Barrett and Hough, 2013). Such sexual dimorphisms usually arise from differential expression of genes between the two sexes, i.e., sex-biased genes (including sex-specific genes expressed exclusively in one sex) that are located on autosomal chromosomes and sex chromosomes/or sex-determining regions (Ellegren and Parsch, 2007; Parsch and Ellegren, 2013; Grath and Parsch, 2016; Charlesworth, 2018; Tosto et al., 2023). Recently, some studies have begun to explore the strength and impact of evolutionary forces that shape different sexually dimorphic traits through sex-biased gene expression (Mank, 2009; Rowe et al., 2018; Naqvi et al., 2019; Cai et al., 2021; Mank, 2023; Murat et al., 2023; Singh and Agrawal, 2023). Previous studies revealed that sex-biased gene expressions were associated with the evolution of sexual dimorphisms in some animal species, although the extent of this bias exhibits great variation among taxa, tissues, and development stages (Mank, 2017; Hsu et al., 2020; Khodursky et al., 2020; Lichilin et al., 2021; Toubiana et al., 2021; Djordjevic et al., 2022; Yue et al., 2023). Unlike most animals, the vast majority (~90%) of flowering plants (angiosperms) are hermaphroditic, while only a small fraction (~5%) are dioecious in which individuals have exclusively male or female reproductive organs (Renner, 2014). Most dioecious plants possess homomorphic sex-chromosomes that

are roughly similar in size when viewed by light microscopy (Palmer et al., 2019). Furthermore, sexual dimorphism in dioecious plants is less common and less conspicuous than in most animals (Barrett and Hough, 2013). Hence, the study of sex-biased gene expression is of great interest to plant evolutionary biologists, as it is necessary to understand the evolution of sexual dimorphism in dioecious plants (Moore and Pannell, 2011).

A common pattern that has emerged from previous studies is that sex-biased genes, particularly male-biased genes, tend to evolve rapidly in protein sequence (the ratio of non-synonymous to synonymous substitutions, d_N/d_S) compared to unbiased genes (Ellegren and Parsch, 2007; Grath and Parsch, 2016). The rapid evolution of male-biased genes was first observed in *Drosophila melanogaster* (Zhang et al., 2004; Zhang and Parsch, 2005) and has been supported by recent investigations in a wider range of animals (Pröschel et al., 2006; Mank et al., 2007; Mank, 2017; Papa et al., 2017; Catalan et al., 2018; Toubiana et al., 2021). In recent years, there have been growing studies on the expression dynamics and molecular evolutionary rates of sex-biased genes in flowering plants, including hermaphroditic *Arabidopsis thaliana* (Gossmann et al., 2014; 2016), *Solanum* (Moyle et al., 2021), and dioecious *Silene latifolia* (Zemp et al., 2016), *Salix viminalis* (Darolti et al., 2018), *Mercurialis annua* (Cossard et al., 2019), *Populus balsamifera* (Sanderson et al., 2019), and *Leucadendron* (Scharmann et al., 2021). However, despite such advances, the molecular evolution pattern of sex-biased genes in plants remains inconsistent among the studied plant species (Muyle, 2019; Veltsos, 2019). In dioecious plants such as

Mercurialis annua and *Leucadendron*, Cossard et al., (2019) and Scharmann et al., (2021) found no significant differences in evolutionary rates of proteins among female-biased, male-biased and unbiased genes detected between male and female plants leaf tissues, although the expression of sex-biased genes was highly different from unbiased genes in leaves. Similar patterns have also been reported in dioecious *Populus balsamifera*, where evolutionary rates of male-biased, female-biased and unbiased genes did not differ in reproductive tissues (Sanderson et al., 2019). However, in the dioecious *Salix viminalis*, male-biased genes have significantly lower evolutionary rates of proteins than female-biased and unbiased genes in catkin tissues (Darolti et al., 2018). To our knowledge, only the five above-mentioned studies have investigated expression differences and protein evolutionary rates of sex-biased genes in dioecious angiosperms. Moreover, these studies only compared gene expression in vegetative versus vegetative tissues and vegetative versus reproductive tissues, limiting our understanding of sexual selection at different floral development stages. Therefore, more studies and taxa are needed to explore the common patterns of sequence evolution in sex-biased genes, with more focus on comparing sex-biased gene expression in reproductive versus reproductive tissues, e.g., different floral development stages in dioecious angiosperms.

Evolutionary analyses indicate that different driving forces impact the rate of sequence evolution of sex-biased genes. These forces include positive selection, which promotes the spread and adaptive fixation of beneficial alleles; sexual selection, which results from male-male competition or female choice; and relaxed

111 purifying selection, which reduces the removal of deleterious mutations (Grath and
112 Parsch, 2016; Mank, 2017; Dapper and Wade, 2020). For example, in animal systems,
113 particularly in *Drosophila*, the elevated sequence divergence rates of male-biased
114 genes have often been interpreted as the signature of adaptive evolution, suggesting
115 that sexual selection is the primary evolutionary force (Pröschel et al., 2006; Assis et
116 al., 2012). In brown algae, female-biased and/or male-biased genes exhibited higher
117 evolutionary rates than unbiased genes, suggesting that rapid evolution is partly
118 driven by adaptive evolution or sexual selection (Lipinska et al., 2015; Cossard et al.,
119 2022; Hatchett et al., 2023). However, studies in plants have never reported elevated
120 rates of sex-biased genes.

121 An alternative explanation for the rapid evolution of sex-biased genes is a
122 relaxation of purifying selection due to reduced constraints (Lahti et al., 2009; Dapper
123 and Wade, 2020). In the model plant *Arabidopsis thaliana*, pollen genes were found to
124 be evolving faster than sporophyte-specific genes due to relaxed purifying selection
125 associated with the transition from outcrossing to selfing (Harrison et al., 2019).
126 These trends were recently confirmed in *Arabis alpina*, which exhibits mating system
127 variation across its distribution, suggesting that the efficacy of purifying selection on
128 male gametophyte-expressed genes was significantly weaker in inbred populations
129 (Gutierrez-Valencia et al., 2022). Together, these findings in plants reinforce the idea
130 that both adaptive (e.g., positive selection, sexual selection) and non-adaptive (e.g.,
131 relaxed selection) evolutionary processes differentially impact the sequence evolution
132 of sex-biased genes. Hence, investigating the potential contribution of selection forces

133 to the emergence of specific evolutionary patterns of sex-biased genes within a focal
134 species is of great interest.

135 In the family Cucurbitaceae, there are about 96 genera and 1,000 species, about
136 50% of species are dioecious, and the others are monoecious (Schaefer and Renner,
137 2011). Phylogenetic analyses of Cucurbitaceae suggest that dioecy is the ancestral
138 state of the family, but transitions frequently to monoecy (Zhang et al., 2006).
139 *Trichosanthes pilosa* (synonym: *T. ovigera*, 2n = 22, Cucurbitaceae) is mainly
140 distributed from Southwest and Southeast China to Japan, extending to Southeast
141 Asia, New Guinea and Western Australia. It was suggested to have originated in the
142 late Miocene (ca. 8-6 million-year ago) (de Boer et al., 2012; 2015; Guo et al., 2020).
143 *Trichosanthes pilosa* is a perennial, night-flowering, insect-pollinated dioecious vine
144 that reproduces sexually and possesses a pair of heteromorphic sex chromosomes
145 XX/XY (Ming et al., 2011). The male parts (e. g., anthers) of female flowers, and the
146 female parts (e. g., pistil and ovaries) of male flowers are fully aborted. However, its
147 male and female flowers exhibit strong sexual dimorphism in floral morphological
148 and phenological traits, such as racemose versus solitary (Fig. 1), early-flowering
149 versus late-flowering, and caducous versus long-lived (Wu et al., 2011).

150 To understand the evolution of sex-biased genes in dioecious *T. pilosa*, we
151 collected floral buds and flowers at anthesis from male and female individuals and
152 characterized their expression profiles using Illumina RNA sequencing. Our primary
153 objectives are to 1) compare expression divergence between males and females at two
154 floral development stages; 2) explore whether there are differences in the evolutionary

155 rates of proteins among female-biased, male-biased and unbiased genes; and if so, 3)
156 determine the main selective forces that contribute to the differentiation of sequence
157 evolution rates among gene categories.

158 **Results**

159 **Transcriptome sequencing, *de novo* assembly and annotation**

160 Using whole transcriptome shotgun sequencing, we sequenced floral buds and
161 flowers at anthesis from female and male of dioecious *T. pilosa*. We set up three
162 biological replicates from three female and three male plants, including 12 samples in
163 total (six floral buds and six flowers at anthesis). We then generated a total of nearly
164 276 million clean reads (Table S1). Due to the absence of a reference genome, we
165 performed *de novo* assembly of transcripts from all the clean reads, followed by
166 clustering and filtering analysis, resulting in 59,051 unigenes (Fig. S1A). To evaluate
167 the quality of the assembled unigenes, we used BUSCO assessments based on
168 embryophyta_odb10 database, which showed the completeness of the reference
169 transcriptome at 89.7% (Table S2). We then annotated them against protein databases
170 including NR, KEGG, Swissport, PFAM, and GO using BLASTP and nucleotide
171 database NT using BLASTN (Table S2). The e-value distribution of the best hits in
172 NR database suggested that 47,241 unigenes (80%) had strong homology, with an e-
173 value smaller than 1.0e-15 (Fig. S1B). The majority of unigenes were annotated by
174 homologs in species of Cucurbitaceae (61.6%, 36,375), such as *Momordica charantia*
175 (16.3%, 9,625), *Cucumis melo* (11.9%, 7,027), *Cucurbita pepo* (11.9%, 7,027),

176 *Cucurbita moschata* (11.5%, 6,791), *Cucurbita maxima* (10.1%, 5,964), and other
177 species (38.4%, 22,676) (Fig. S1C). Overall, our assessment suggested that we have
178 generated high-quality reference transcriptomes.

179 **Expression characteristics of sex-biased genes**

180 We mapped the RNA-Seq reads of floral buds and flowers at anthesis onto the
181 reference transcriptome in dioecious *T. pilosa*, which resulted in approximately 75%
182 read mappings per sample (Table S3). In floral buds, we identified 5,096 (9.50%)
183 female-biased genes and 4,214 (7.86%) male-biased genes (Fig. 2A). In contrast, only
184 380 (0.70%) female-biased genes and 233 (0.43%) male-biased genes were detected
185 in flowers at anthesis (Fig. 2B). Using hierarchical clustering analysis, we evaluated
186 different levels of gene expression across sexes and tissues (Fig. 2C), revealing that
187 female floral buds maybe tend to masculinize, and vice versa in the early stages of
188 floral development. Furthermore, we observed that the number of sex-biased genes in
189 floral buds was approximately 15 times higher than in flowers at anthesis, indicating
190 that sex-biased genes associated with meiotic processes, sex differentiation and
191 sexually dimorphic traits are predominantly expressed in floral buds. We also
192 analyzed sex-specific genes that were exclusively expressed in floral buds and flowers
193 at anthesis of one sex. In floral buds, we found 253 out of 5,096 (4.96%) female-
194 specific genes and 465 out of 4,214 (11.03%) male-specific genes. However, in
195 flowers at anthesis, we only identified 26 out of 380 (6.84%) female-specific genes
196 and 52 out of 233 (22.32%) male-specific genes. Taken together, sex bias is more

197 prevalent in floral buds than in flowers at anthesis.

198 **Tissue-biased/stage-biased gene expression**

199 We compared the expression levels of transcripts in floral buds and flowers at
200 anthesis within each sex to identify genes with tissue-biased expression. In male
201 plants, the number (M2TGs: n = 2,795) of tissue-biased genes in male flowers at
202 anthesis (M2TGs) was 1,040 higher than that in male floral buds (M1TGs: n = 1,755,
203 Fig. 3A and 3B). However, in female plants, the number (F2TGs: n = 660) of tissue-
204 biased genes in female flowers at anthesis (F2TGs) was only 536 more than that in
205 female floral buds (F1TGs: n = 124, Fig. 3C and 3D). Our results indicated that males
206 had a higher tissue-bias relative to females. We also identified sex-biased genes that
207 were expressed in both types of tissues by comparing tissue-biased genes with male-
208 biased and female-biased genes, respectively. Few female-biased genes in floral buds
209 (F1BGs: n = 5,096) overlapped with tissue-biased genes in female floral buds
210 (F1TGs: n = 124) and female flowers at anthesis (F2TGs: n = 660), accounting for
211 only 85 out of 5,096 (1.67%) (Fig. 3C). Similarly, few female-biased genes in flowers
212 at anthesis (F2BGs: n = 380) overlapped with tissue-biased genes in female floral
213 buds (F1TGs: n = 124) and female flowers at anthesis (F2TGs: n = 660), occupying
214 around 5 out of 380 (1.32%) (Fig. 3D). However, a significant proportion of male-
215 biased genes in floral buds (M1BGs: n = 4,214) overlapped with tissue-biased genes
216 in male floral buds (M1TGs: n = 1,755) and male flowers at anthesis (M2TGs: n =
217 2,795), with 1,010 out of 4,214 (23.97%) (Fig. 3A). A high proportion of male-biased

genes in flowers at anthesis (M2BGs: n = 233) overlapped with tissue-biased genes in male floral buds (M1TGs: n = 1,755) and male flowers at anthesis (M2TGs: n = 2,795), 145 out of 233 (62.23%) (Fig. 3B).

Elevated protein evolutionary rates of male-biased genes in floral buds

We compared rates of protein evolution among male-biased, female-biased and unbiased genes in four species with phylogenetic relationships (((*T. anguina*, *T. pilosa*), *T. kirilowii*), *Luffa cylindrica*), including dioecious *T. pilosa*, dioecious *T. kirilowii*, monoecious *T. anguina* in *Trichosanthes*, together with monoecious *Luffa cylindrica*. To do this, we sequenced transcriptomes of *T. pilosa.* We also collected transcriptomes of *T. kirilowii*, as well as genomes of *T. anguina* and *Luffa cylindrica* (see Methods Section). We identified 1,145 female-biased, 343 male-biased, and 2,378 unbiased one-to-one orthologous groups (OGs) from floral buds. Additionally, we detected 45 female-biased, 13 male-biased, and 3,782 unbiased one-to-one OGs from mature flowers in all four species. To quantify the rates of protein sequences, we separately calculated ω values for each sex-biased and unbiased orthologous gene using 'two-ratio' and 'free-ratio' branch models in juvenile and mature flowers (Figs. 4 and S2).

The two-ratio branch model, where the foreground (dioecious branches) has a different ω value relative to the background (all other branches), is better supported than the fixed-ratio branch model, where all branches are constrained to have the same ω value. In the results of the 'two-ratio' branch model, the median of ω values in

239 female-biased, male-biased and unbiased genes were 0.227, 0.257 and 0.230 in floral
240 buds, respectively (Fig. 4A and Table S4). We observed that male-biased genes had a
241 13.22% and 11.74% higher median than female-biased and unbiased genes in floral
242 buds, respectively. The difference in the distribution of ω values between female-
243 biased versus male-biased genes (P = 0.0021) and male-biased versus unbiased genes
244 (P = 0.0051) was statistically significant in Wilcoxon rank sum tests. However, we
245 did not find a significant difference in ω values between female-biased and unbiased
246 genes in floral buds (Wilcoxon rank sum test, P = 0.4618). In flowers at anthesis, the
247 median of ω values for female-biased, male-biased, and unbiased genes were 0.269,
248 0.177 and 0.231, respectively (Fig. 4B and Table S4). However, there was no
249 statistically significant difference in the distribution of ω values using Wilcoxon rank
250 sum tests for female-biased versus male-biased genes (P = 0.0556), female-biased
251 versus unbiased genes (P = 0.0796), and male-biased versus unbiased genes (P =
252 0.3296) possibly because of limited statistical power due to the low number of sex-
253 biased genes in flowers at anthesis.

254 In free-ratios model, ω values are free to vary in each branch compared to fixed-
255 ratio branch model and two-ratio branch model. The 'free-ratio' branch model yielded
256 interesting results. In floral buds, the median ω values for female-biased, male-biased,
257 and unbiased genes were 0.222, 0.265 and 0.226, respectively (Fig. 4C and Table S5).
258 Male-biased genes had a significantly higher median relative to female-biased genes
259 (19.37% higher, Wilcoxon rank sum test, P = 0.0009) and unbiased genes (17.26%
260 higher, Wilcoxon rank sum test, P = 0.0004) in floral buds. However, there was no

261 significant difference in ω values between female-biased and unbiased genes
262 (Wilcoxon rank sum test, $P = 0.9862$). In flowers at anthesis, the median ω values for
263 female-biased, male-biased, and unbiased genes were 0.300, 0.148 and 0.227,
264 respectively (Fig. 4D and Table S5). Female-biased and unbiased genes had
265 significantly higher ω values than male-biased (Wilcoxon rank sum test, $P = 0.0101$,
266 $P = 0.0146$, respectively). However, there was no significant difference in ω values
267 between female-biased and unbiased genes (Wilcoxon rank sum test, $P = 0.2887$).
268 Since the number of male-biased genes and evolutionary rates of male-biased genes in
269 flowers at anthesis are lower than those in floral buds, we decided to focus on the
270 latter in subsequent analyses. Additionally, we also ran permutation t test, which is
271 almost consistent with the results of Wilcoxon rank sum test. We found that only in
272 floral buds, there were significant differences in ω values in the results of 'free-ratio'
273 model (female-biased versus male-biased genes, $P = 0.04282$ and male-biased versus
274 unbiased genes, $P = 0.01114$) and 'two-ratio' model (female-biased versus male-
275 biased genes, $P = 0.01992$ and male-biased versus unbiased genes, P = 0.02127,
276 respectively).

277 **Evidence of positive selection and relaxed selection for male-biased genes in**
278 **floral buds**

279 After comparing classical branch-site model A and branch-site model null
280 models (see Methods Section), we discovered that 39 out of 343 OGs (11.34%) in
281 male-biased genes of floral buds exhibited strong evidence of having certain sites that

evolved under positive selection based on foreground ω value, likelihood ratio tests (LRTs, $P < 0.05$) and Bayes empirical Bayes (BEB) value (Fig. 5 and Table S6). As a complementary approach, we utilized the aBSREL and BUSTED methods that are implemented in HyPhy v.2.5 software, which avoids false positive results by classical branch-site models due to the presence of rate variation in background branches, and detected significant evidence of positive selection. According to our findings, 84 out of 343 OGs (24.49%) were identified to be under episodic positive selection in male-biased genes of floral buds with a site proportion of 0.17%–26.44% based on aBSREL (Table S7). In addition, 69 out of 343 OGs (20.01%) exhibited significant signs of positive selection with the site proportion of 0.28%–32.65% in male-biased genes of floral buds according to BUSTED (Table S8). Among these, a total of 32 OGs (9.30%) were identified through our tests using CodeML, aBSREL and BUSTED (Fig. 5).

Relaxed selection may occur when the efficiency of natural selection (e.g., the reduction of the strength of purifying selection) is reduced, leading to accumulations of deleterious mutations (Lahti et al., 2009; Dapper and Wade, 2020). This has been proposed as an explanation for the rapid evolution of sex-biased genes (Lahti et al., 2009; Mank, 2017). Using the RELAX model, we conducted an analysis and detected that 18 out of 343 OGs (5.23%) showed significant evidence of relaxed selection (K = 0.0184–0.6497) (Tables S9). We also found that most of them were members of different gene families generated by gene duplication (Table S13). Additionally, we observed that 61 out of 343 OGs (17.73%) exhibited significant evidence of

304 intensified positive selection (K = 2.3363–50, $\omega_2 \geq 1$) (Fig. 5 and Table S10), which is
305 consistent with the results obtained from CodeML, aBSREL and BUSTED.
306 According to previous studies (Ellegren and Parsch, 2007; Catalan et al., 2018),
307 genes that exhibit sex-biased expression with rapid evolutionary rates tend to display
308 a lower codon bias compared to unbiased genes. In our results, we found that male-
309 biased genes in floral buds had a significantly lower median effective number of
310 codons (ENCs) than both female-biased and unbiased genes (Wilcoxon rank sum test,
311 female-biased vs male-biased genes, $P = 0.0001$ and male-biased vs unbiased genes,
312 $P = 0.0123$). This suggested that male-biased genes in floral buds exhibit stronger
313 codon bias than both female-biased and unbiased genes (Fig. S3). Similarly, given
314 that d_N/d_S values of sex-biased genes were higher due to codon usage bias, lower d_S
315 rates would be expected in sex-biased genes relative to unbiased genes (Ellegren &
316 Parsch, 2007; Parvathy et al., 2022). However, we exhibited that the median of d_S
317 values in male-biased genes were much higher than those in female-biased and
318 unbiased genes in the results of 'free-ratio' (Fig. S4A, female-biased versus male-
319 biased genes, $P = 6.444e-12$ and male-biased versus unbiased genes, $P = 4.564e-13$)
320 and 'two-ratio' model (Fig. S4B, female-biased versus male-biased genes, $P = 2.2e-16$
321 and male-biased versus unbiased genes, $P = 9.421e-08$, respectively). In short, our
322 analyses indicated that rapid evolutionary rates of male-biased genes in floral buds
323 were not associated with a reduction in codon usage bias.
324 We also analyzed female-biased and unbiased genes that underwent positive and
325 relaxed selection in floral buds (Tables S6-S10). We identified 216 (18.86%)

326 positively selected (Fig. S5), and 69 (6.03%) relaxed selective female-biased genes
327 from 1,145 OGs, respectively. Similarly, we found 436 (18.33%) positively selected
328 (Fig. S6), and 43 (1.81%) unbiased genes under relaxed selection from 2,378 OGs,
329 respectively. Notably, male-biased genes have a higher proportion (10%) of positively
330 selected genes compared to female-biased and unbiased genes. However, relaxed
331 selective male-biased genes have a higher proportion (3.24%) than unbiased genes,
332 but about 0.8% lower than that of female-biased genes. In summary, our analyses
333 suggested that positive selection and relaxed selection likely drove the rapid
334 evolutionary rates of male-biased genes compared to female-biased and unbiased
335 genes in floral buds.

336 **Functional analysis of sex-biased genes in floral buds**

337 We conducted KEGG pathway enrichment analysis on sex-biased genes in floral
338 buds. Our results showed that 699 genes were female-biased and 358 genes were
339 male-biased, with significant enrichment ($P < 0.05$) in 26 and 24 KEGG pathways,
340 respectively (Table S11). In the floral bud stage, we observed that female-biased
341 genes were mainly enriched in metabolic and signaling pathways, such as ribosome,
342 Fatty acid elongation, photosynthesis and plant hormone signal transduction (Fig. S7A
343 and Table S11). On the other hand, male-biased genes were significantly enriched in
344 metabolic and signaling pathways, including inositol phosphate metabolism, starch
345 and sucrose metabolism, regulation of autophagy, plant hormone signal transduction,
346 and Toll-like receptor signaling pathway (Fig. S7B and Table S11).

We have also found that certain male-biased genes, which are evolving under positive selection and relaxed selection (Table S12 and S13), were related to abiotic stress and immune responses. For instance, mitogen-activated protein kinase kinase kinase 18 (MAPKKK18) (Zhang and Zhang, 2022), zinc finger CCCH domain-containing protein 20 (C3H20/TZF2) (Bogamuwa and Jang, 2014), and heat stress transcription factor B-3 (HSFB3) (Scharf et al., 2012) have been linked to stress. Additionally, ten male-biased genes with rapid evolutionary rates were associated with anther and pollen development. These genes include LRR receptor-like serine/threonine protein kinase (LRR-RLK) (Cui et al., 2022), pollen receptor-like kinase 3 (*PRK3*) (Muschietti and Wengier, 2018), autophagy-related protein 18f (*ATG18f*) (Zhou et al., 2015; Li et al., 2020), and plant homeodomain (PHD) finger protein 3 (*MALE STERILITY 3*) (Hou et al., 2022) in floral buds of male plants.

Discussion

The Cucurbitaceae family, where half of the species are monoecious and half are dioecious, is an excellent model for studying the evolution of sexual systems of angiosperms, including sex-determination mechanism and sexual dimorphism (Schaefer and Renner, 2010; Boualem et al., 2015; Ma and Pannell, 2016). In this study, we aimed to investigate whether sex-biased genes exhibited evidence of rapid evolutionary rates of protein sequences and identify the evolutionary forces responsible for the observed patterns in the dioecious *Trichosanthes pilosa*. We compared the expression profiles of sex-biased genes between sexes and two tissue

368 types and examined the signatures of rapid sequence evolution for sex-biased genes,
369 as well as the contributions of potential evolutionary forces.

370 **Sex-biased expression in floral buds**

371 Several studies have shown that in dioecious plants, male-biased genes tend to
372 outnumber female-biased genes, consistent with the patterns in most animals (Zhang
373 et al., 2007; Djordjevic et al., 2022). For instance, insect-pollinated dioecious plants
374 such as *Asparagus officinalis* (Harkess et al., 2015) and *Silene latifolia* (Zemp et al.,
375 2016), exhibit a higher proportion of male-biased genes. In contrast, the wind-
376 pollinated dioecious plant *Populus balsamifera* (Sanderson et al., 2019) has twice as
377 many female-biased genes as male-biased genes. The differences in these studies
378 could be partly attributed to the impact of sexual selection on secondary sexual traits
379 in insect-pollinated dioecious plants, as opposed to wind-pollinated ones (Delph and
380 Herlihy, 2012; Muyle, 2019; Sanderson et al., 2019). Similar to the above study of
381 *Populus balsamifera*, our findings revealed that the number of female-biased genes in
382 floral buds of the night-flowering, insect-pollinated dioecious plant *Trichosanthes*
383 *pilosa* exceeded that of male-biased genes by 882 (~21%). This excess of female-
384 biased expression could be due to lower energy consumption needs and reduced
385 chemical defence capability against insect herbivores in short-lived male flowers
386 (Sanderson et al., 2019). Indeed, functional enrichment analysis in chemical pathways
387 such as terpenoid backbone and diterpenoid biosynthesis indicated that relative to
388 male floral buds, female floral buds had more expressed genes that were equipped to

389 defend against herbivorous insects and pathogens, except for growth and development
390 (Vaughan et al., 2013; Ren et al., 2022) (Fig. S7A and Table S11). Additionally, our
391 enrichment analysis showed that the photosynthesis, porphyrin and chlorophyll
392 metabolism pathways were more active in female floral buds compared to male floral
393 buds (Fig. S7A and Table S11), enabling them to acquire more resources such as
394 carbon for fruit and seed production (Delph,1999).

395 We identified functional enrichments in Toll-like receptor signaling, NF-kappa B
396 signaling, and inositol phosphate metabolism pathways in male floral buds (Fig. S7B,
397 Table S11). We also found that male-biased genes with high evolutionary rates in male
398 floral buds were associated with functions to abiotic stresses and immune responses
399 (Tables S12 and S13), which suggest that male floral buds through rapidly evolving
400 genes are adapted to mountain climate and the environment in Southwest China
401 relative to female floral buds through high gene expression. In addition, the
402 enrichment in regulation of autophagy pathways could be associated with gamete
403 development and the senescence of male floral buds (Table S14) (Liu and Bassham,
404 2012; Li et al., 2020; Zhou et al., 2021). In fact, it was observed that male flowers
405 senesced faster (Wu et al., 2011). We also found that homologous genes of two male-
406 biased genes in floral buds (Table S14) that control the raceme inflorescence
407 development (Teo et al., 2014) were highly expressed compared to female floral buds.
408 Taken together, these results indicate that expression changes in sex-biased genes,
409 rather than sex-specific genes play different roles in sexual dimorphic traits in
410 physiology and morphology (Dawson and Geber, 1999).

411 **Rapid Evolution of male-biased genes in floral buds**

412 It has been observed that, in most animals, sex-biased genes, particularly those
413 biased towards males, often exhibit more rapid evolutionary rates than unbiased genes
414 (Parsch and Ellegren, 2013; Grath and Parsch, 2016; Mank, 2017; Toubiana et al.,
415 2021). However, in dioecious angiosperms, no evidence of rapid evolution in sex-
416 biased genes relative to unbiased genes has been found (Zemp et al., 2016; Darolti et
417 al., 2018; Cossard et al., 2019; Sanderson et al., 2019; Scharmann et al., 2021). In
418 contrast, our findings indicated that male-biased genes experience higher evolutionary
419 rates than both female-biased and unbiased genes in floral buds of dioecious *T. pilosa.*
420 We proposed that positive selection and relaxed purifying selection may be
421 responsible for the rapid sequence evolution of male-biased genes.

422 After analyzing the data, we found that around 28.57% (98 genes) of male-biased
423 genes have undergone positive selection. Additionally, we observed that the
424 proportion of male-biased genes under positive selection was about 10% higher than
425 that of female-biased and unbiased genes. Furthermore, we discovered that some
426 male-biased genes under positive selection were linked to abiotic stress and immune
427 responses (Table S12). Our findings are consistent with studies on *Drosophila* and
428 *Ectocarpus* (Zhang and Parsch, 2005; Lipinska et al., 2015), suggesting that adaptive
429 evolution is one of the important driving forces for rapid evolutionary rates. Notably,
430 we identified several male-biased genes under positive selection that are functionally
431 related to early flowering (*phyB*) (Stephenson and Bertin, 1983; Forrest, 2014; Hajdu
432 et al., 2015) and pollen development (Skogsmyr and Lankinen, 2002; Williams and

433 Reese, 2019) (Tables S12-S14). These findings indicate that a small fraction of male-
434 biased genes may experience adaptive evolution due to sexual selection, driven by
435 male-male competition.

436 Alternatively, relaxed constraints could contribute to the rapid evolutionary rates
437 of sex-biased genes through three key characteristics (Dapper and Wade, 2020; Tosto
438 et al., 2023). First, sex-biased genes are often expressed solely in reproductive tissues
439 of one sex (e.g., sex-specific genes), particularly in the haploid phase (Sandler et al.,
440 2018; Immler, 2019; Beaudry et al., 2020). Sex-specific selection (e.g., relaxed
441 purifying selection) acting on sex-specific genes could decrease the elimination of
442 deleterious mutations (Mank, 2017), such as pollen-specific (Harrison et al., 2019) or
443 testes-specific genes (Gershoni and Pietrokovski, 2014). However, we observed male-
444 biased genes but not male-specific genes undergoing relaxed purifying selection.
445 Second, sex-biased genes are often expressed in few tissues (tissue-biased genes)
446 (Meisel, 2011; Tosto et al., 2023), resulting in these genes rapidly evolving under
447 positive selection or relaxed purifying selection due to low evolutionary constraints
448 (Congrains et al., 2018; Whittle et al., 2021; Tosto et al., 2023). In our results, 343
449 male-biased genes (M1-biased genes, M1BGs) with faster evolutionary rates relative
450 to female-biased and unbiased genes overlapped with 1,755 tissue-biased genes in
451 floral buds (M1-tissue-biased genes, M1TGs) (27 out of 343, 7.87%) (Fig. S8A).
452 Furthermore, 27 out of 343 male-biased genes (that is, tissue-biased genes) in floral
453 buds overlapped with nine out of 98 (9.18%) male-biased genes under positive
454 selection (Fig. S8B), and one out of 18 (5.56%) male-biased genes under relaxed

455 purifying selection (Fig. S8C). So, we obtained ten rapidly evolving tissue-biased
456 genes which were also male-biased in male flower buds, suggesting that elevated
457 evolutionary rates may partly be linked to low constraints, consistent with male-
458 biased genes in *Anastrepha* and *Fucus* (Congrains et al., 2018; Hatchett et al., 2023).
459 Finally, gene duplication has long been thought to promote functional divergences and
460 phenotypic novelties by relaxing the constraints of purifying selection on the
461 duplicated gene copy early in its history (Lynch and Conery, 2000; Lynch and Katju,
462 2004; Lahti et al., 2009). For instance, the progesterone receptor gene family in the
463 human lineage (Marinić and Lynch, 2020) and the CYP98A9 clade in Brassicales (Liu
464 et al., 2016) have demonstrated rapid evolution and divergent function due to relaxed
465 purifying selection. In our results, we identified 18 out of 343 (5.25%) male-biased
466 genes that underwent relaxed purifying selection using RELAX model (Table S13).
467 Interestingly, the vast majority of genes under relaxed selection were members of
468 different gene families generated by gene duplication (including whole-genome
469 duplication), such as LOB domain-containing protein 18 (*LBD18*) (Zhang et al.,
470 2020), WRKY transcription factor 72 (*WRKY72*) (Chen et al., 2017), and pollen
471 receptor-like kinase 3 (*PRK3*) (Muschietti and Wengier, 2018).
472 Additionally, reducing codon usage bias could theoretically accelerate
473 evolutionary rates of sex-biased genes by decreasing synonymous substitution rates.
474 However, our results did not support this idea due to stronger codon usage bias in
475 male-biased genes (Fig. S3). Codon usage bias is influenced by many factors, such as
476 levels of gene expression. Highly expressed genes have a stronger codon usage bias

477 and could be encoded by optimal codons for more efficient translation (Frumkin et al.,
478 2018; Parvathy et al., 2022), consistent with high levels of gene expression in males
479 (that is, male-biased genes) in floral buds. Additionally, stronger codon usage bias
480 may be related to higher synonymous substitution rates (Parvathy et al., 2022).
481 Indeed, male-biased genes had significantly higher median *d*s values than female-
482 biased and unbiased genes, both in the 'free-ratio' analysis (Fig. S4A) and 'two-ratio'
483 branch model (Fig. S4B).

484 Several species have been observed to exhibit rapid evolutionary rates of
485 sequences on sex chromosomes compared to autosomes, which has been related to the
486 evolutionary theories of fast-X or fast-Z (Meisel and Connallon, 2013; Hough et al.,
487 2014; Wright et al., 2015; Charlesworth et al., 2018; Darolti et al., 2023).
488 Furthermore, the quantification of gene expression by bulk RNA-seq technology,
489 relative to single-cell transcriptome analysis, has been shown to potentially obfuscate
490 true signals in the evolution of sex-biased gene expression in complex aggregations of
491 diverse cell types (Darolti and Mank, 2023; Tosto et al., 2023). Additionally, our
492 samples were relatively small, and may provide low power to detect differential
493 expression and evolutionary analysis. Therefore, investigation of these interesting
494 issues related to sex-biased gene evolution in *T. pilosa* can only be conducted when
495 whole genome sequences and population datasets become available in the near future.

496 **Methods**

497 **Plant materials and RNA isolation**

498 Floral buds (≤ 3 mm) and flowers at anthesis were sampled from three female
499 and three male plants (Fig. 1) from the mountainous regions of Anning (Qinglong
500 Gorge), Yunnan Province in Southwest China. Floral buds from female and male
501 plants were named F1 and M1, respectively. Similarly, flowers at anthesis from
502 female and male plants, there were named F2 and M2, respectively (Table S1). To
503 exclude possible bacterial contamination, all tissues were sterilized with 75% alcohol
504 and immediately rinsed with purified water. All samples were then snap-frozen in
505 liquid nitrogen, and stored at -80˚C. Total RNA was extracted from each sample using
506 TRIzol reagent (Life Technologies, CA, USA) according to the manufacturer's
507 instructions. The quantification and qualification of RNA were assessed by the RNA
508 Nano 6000 Assay Kit of the Bioanalyzer 2100 system (Agilent Technologies, CA,
509 USA).

510 **Illumina sequencing, *de novo* assembly and annotation**

511 To construct the library, approximately 2 μg of total RNA was used with the
512 Illumina NEBNext UltraTM RNA Library Prep Kit. RNA sequencing was performed
513 on the Illumina NovaSeq 6000, generating 150 bp paired-end reads. The resulting
514 clean reads were obtained by removing adapters, reads containing N bases and low-
515 quality reads using Trimmomatic v.0.39 (Bolger et al., 2014). These reads were

516 deposited in the NCBI database (PRJNA899312).

517 *De novo* assembly for clean reads from all samples was performed using Trinity
518 v.2.10.0 (Haas et al., 2013) with min_kmer_cov: 3 and all other default parameters. To
519 eliminate contamination, all transcripts of *de novo* assembly were compared to
520 bacterial genomes downloaded from NCBI databases using BLASTN with e-value of
521 1.0e-05 in blast+ 2.12.0 software. We used Corset v.4.6 (Davidson and Oshlack, 2014)
522 to obtain high quality, non-redundant consensus transcripts (unigenes). TransDecoder
523 v.5.5.0 was run with -m 100 parameters, namely at least 100 amino acids, to predict
524 the coding DNA and protein sequences (Haas et al., 2013).

525 To evaluate the accuracy and completeness of reference transcriptomes, we
526 performed gene function annotations based on the following databases, using BLAST
527 with a cutoff e-value of 1.0e-05: NR, NT and Swissport (Shiryev et al., 2007). We
528 mapped the unigenes to Pfam database using InterProScan v.5.41 (Jones et al., 2014),
529 to the GO database using Blast2GO (Conesa et al., 2005), and to the KEGG database
530 using KEGG automatic annotation server (Moriya et al., 2007). Additionally, we
531 estimated the completeness of reference transcriptomes using BUSCO v.5.4.5 based
532 on embryophyta_odb10 database (Seppey et al., 2019).

533 **Detection of sex-biased genes**

534 Clean reads were mapped onto all unigenes using Bowtie2 (Langmead and
535 Salzberg, 2012). Read counts were normalized to FPKM (Fragments Per Kilobase
536 Million) value for each unigene using RSEM (Li and Dewey, 2011) in different male

537 and female samples. Genes with zero read counts (i.e., no expression) in both two
538 sexes and tissues were excluded. Differential expression analysis between sexes and
539 tissue types was performed using DESeq2 R package (Love et al., 2014). Unigenes
540 with an FDR-adjusted $P < 0.05$ and an absolute value of $\log_2$ ratio ≥ 1 identified by
541 DESeq2 were considered as sex-biased genes. To perform KEGG functional
542 enrichment, we used all KEGG annotation terms for all genes as the background and
543 performed the analyses using KOBAS v.2.0.12 (Mao et al., 2005).

544 **Evolutionary rate analyses**

545 To quantify the evolutionary rates of sex-biased genes, we download published
546 genome datasets for monoecious *Trichosanthes anguina* (Ma et al., 2020) and
547 monoecious *Luffa cylindrica* which has a closer phylogenetic relationship with
548 *Trichosanthes* (de Boer et al., 2012; Wu et al., 2020) from CuGenDB database (Zheng
549 et al., 2019). Additionally, we also download published RNA sequencing reads of
550 floral buds and flowers from CNCB (Accession CRA002313) and NCBI databases
551 (Accession SRR5259239) for dioecious plant *Trichosanthes kirilowii* (Hu et al.,
552 2020), and *de novo* assembled by previously described methods.
553 We identified one-to-one OGs using OrthoFinder v.2.3.3 with default parameters
554 from *T. anguina*, *T. pilosa*, *T. kirilowii*, and *Luffa cylindrica* (Emms and Kelly, 2019).
555 Then, we employed TranslatorX with -c 1 -p M -g -b5 n parameters (i.e., the multiple
556 alignment and the trimming using Muscle and GBlocks, respectively), translated
557 nucleotide sequences and back-translated amino acid alignments into nucleotide

558 alignments to ensure codon-to-codon alignment (Abascal et al., 2010). The remaining
559 gapless alignments (≥100 bp in length) were retained.

560 To investigate the evolutionary rates of coding sequences, we estimated
561 nonsynonymous substitution (d_N), synonymous substitution (d_S) rates, as well as
562 protein substitution rates (d_N/d_S, ω), using two branch models from CodeML package
563 in PAML v.4.9h with the F3x4 codon frequencies (CodonFreq = 2) (Yang, 2007).
564 According to the phylogenetic relationships of *Trichosanthes* (de Boer et al., 2012;
565 Guo et al., 2020), we set up tree structures ((*T. anguina*, *T. pilosa*), *T. kirilowii*, *L.*
566 *cylindrica*) in the control file of CodeML. First, we employed a 'two-ratio' branch
567 model (model = 2, Nssites = 0) that assumes the foreground (two dioecious species)
568 has a different ω value from the background (two monoecious species) to estimate and
569 compare the divergences of the foreground. Second, to reduce the potential bias of ω
570 value due to the conflation of two dioecious species, we also implemented a 'free-
571 ratio' branch model (model = 1, Nssites = 0), which assumes an independent ω ratio
572 for each branch. Finally, to avoid the effects of saturation substitution, we used
573 separately OGs with $0 < \omega < 2$ and all OGs with $\omega > 0$, plotted the distribution of ω
574 values and compared the median of ω values in female-biased, male-biased and
575 unbiased orthologous genes of floral buds and flowers at anthesis. All comparisons
576 between sex-biased and unbiased genes were tested using Wilcoxon rank sum test in
577 R software. Additionally, we also performed permutations t-tests with 100,000
578 permutations in the R package Deducer (Fellows, 2012).

579 **Estimation of the strength of natural selection**

580 The rapid evolutionary rates of sex-biased genes may be attributed to positive
581 selection, relaxed selection and lower codon usage bias (Catalan et al., 2018; Dapper
582 and Wade, 2020). Therefore, we conducted separate analyses using classical branch-
583 site models that assume different ω values both among branches and across sites
584 (Álvarez-Carretero et al., 2023), the adaptive branch-site random effects likelihood
585 (aBSREL) model (Smith et al., 2015), the branch-site unrestricted statistical test for
586 episodic diversification (BUSTED) model (Murrell et al., 2015), the RELAX model
587 (Wertheim et al., 2015), and the effective number of codons (ENC) in PAML v.4.9h
588 (Yang, 2007), HyPhy v.2.5 (Pond et al., 2020) and CodonW v.1.4.2
589 (http://codonw.sourceforge.net) to distinguish which evolutionary forces are driving
590 the rapid evolutionary rates of sex-biased genes.

591 To determine if amino acid sites in the foreground, including the *T. pilosa* lineage
592 have undergone positive selection (foreground ω >1) compared with the background
593 for each OGs, we followed the steps of Zhang et al. (2005), and used branch-site
594 model A (model = 2, Nssite = 2, fix_omega = 0, omega = 1.5) and branch-site model
595 null (model = 2, Nssite = 2, fix_omega = 1, omega = 1). The classical branch-site
596 model assumes four site classes (0, 1, 2a, 2b), with different ω values for the
597 foreground and background branches. In site classes 2a and 2b, the foreground branch
598 undergoes positive selection when there is ω > 1. We examined the significance of
599 likelihood ratio tests (LRTs, $P < 0.05$) to identify positively selected sites between
600 model A and model null by comparing LRTs to the Chi-square distribution with two

601 degrees of freedom. We adjusted the LRTs *P* value for multiple comparisons using
602 Benjamini and Hochberg's (FDR) algorithm. When the *P* value was significant, we
603 used Bayes Empirical Bayes (BEB) estimates to identify sites with a high posterior
604 probability (pp ≥ 0.95) of being under positive selection (Yang et al., 2005).
605 To detect episodic positive selection at a proportion of sites on the foreground
606 branch, we employed the aBSREL method (Smith et al., 2015) in the HyPhy v.2.5
607 packages to compare the fully adaptive model ($\omega > 1$) to the null model that allows no
608 positive selection rate classes by LRTs, which is an improved algorithm of branch-site
609 models in PAML. For relatively small datasets, such as those with fewer than 10 taxa,
610 the aBSREL method may not have enough power to detect positive selection.
611 Therefore, we also ran the BUSTED method to identify gene-wide evidence of
612 episodic positive selection at least one site on at least one branch (Murrell et al.,
613 2015). We set *T. pilosa* as the foreground and assessed the statistical significance ($P <$
614 0.05) using LRTs with the Holm-Bonferroni correction.
615 To test the relaxation of selective strength, we utilized the RELAX model in the
616 HyPhy v.2.5 software (Wertheim et al., 2015; Schrader et al., 2021). The RELAX
617 model estimates three ω parameters ($\omega_0 \leq \omega_1 \leq 1 \leq \omega_2$), and determines the proportion
618 of sites in the test (foreground) and reference (background) branches using a branch-
619 site model. The first two ω classifications indicate that sites have undergone purifying
620 selection, and the third classification indicates that sites have been under positive
621 selection. Additionally, the model introduces a selection intensity parameter (K value)
622 to compare a null model (K = 1) with an alternative model, thereby assessing the

strength of natural selection. When K > 1, it suggests intensified natural selection, when K < 1, indicates relaxed natural selection in the test branch relative to the reference branch. We quantified the statistical confidence of K value ($P < 0.05$) using LRTs and the Holm-Bonferroni correction.

To investigate codon usage bias, which refers to the differences in the frequency of occurrence of synonymous codons in coding DNA, we employed CodonW v.1.4.2. This program considers the ENC values from 20 to 61 as a measure of the departure of the genetic codes for a given gene (Wright, 1990), with lower ENC values represent stronger codon usage bias (Hambuch and Parsch, 2005). We performed a Wilcoxon rank sum test to determine if there were deviations in ENC values among female-biased, male-biased, and unbiased genes in floral buds.

Acknowledgements

We are very grateful to Spencer C. H. Barrett (University of Toronto, Canada) for his critical reading and suggestions on the manuscript. We also thank three anonymous reviewers for their comments on improving the quality of the manuscript. We are indebted to Ting Zhang, Zhi-Yun Yang, Jiang-Li Ma, Peng-Fei Ma, Xu-Kun Wu, Shi-Yu Lv, Zhen Peng and other members of staff of Germplasm Bank of Wild Species for sampling. We also thank the iFlora HPC Center (iFlora High Performance Computing Center) of Germplasm Bank of Wild Species for computational support on data analysis.

Funding

This study was funded by the Strategic Priority Research Program of the Chinese Academy of Sciences, China (XDB31000000), the National Natural Science Foundation of China (32370233, 31570333), the Key R and D Program of Yunnan Province, China (202103AC100003), the Key Basic Research Program of Yunnan Province, China (202101BC070003), the Science and Technology Basic Resources Investigation Program of China (2019FY100900), and the open research project of "Cross-Cooperative Team" of the CAS' Germplasm Bank of Wild Species, Kunming Institute of Botany. The study was also supported by the National Wild Plant Germplasm Resource Center and the CAS Key Technology Talent Program.

Author contributions

HTL, DZL and LZ conceived the project the study. HTL and LZ designed and performed the experiment. LZ, JH and HTL collected the samples. LZ analyzed the data and wrote the manuscript. HTL, DZL, LZ, and WZ revised the manuscript. All authors approved the final manuscript.

Additional files

Supplementary files

Supplementary file 1. Supplementary Figures S1 to S8.

Supplementary Figure S1. The length distribution of unigenes (A) and the e-value distribution (B) and the species distribution (C) of BLAST hits for each unigene.

Supplementary Figure S2. Boxplot of d_N/d_S values (including all ω values) of female-biased, male-biased and unbiased genes in floral buds and flowers at anthesis of *Trichosanthes pilosa*. White dot indicates the median of dN/dS values for sex-biased and unbiased genes. Wilcoxon rank sum tests are used to test for significant differences (***$P < 0.0005$, **$P < 0.005$ and *$P < 0.05$). The distributions of d_N/d_S values for female-biased, male-biased and unbiased genes in floral buds (A) and flowers at anthesis (B) using 'free-ratio' branch model. The distributions of d_N/d_S values for female-biased, male-biased and unbiased genes in floral buds (C) and flowers at anthesis (D) using 'two-ratio' branch model.

Supplementary Figure S3. Violin plots of ENCs values of female-biased, male-biased and unbiased genes in floral buds. Significant differences using Wilcoxon rank sum tests are represented by * (***$P < 0.0005$ and *$P < 0.05$).

Supplementary Figure S4. Boxplot of d_S values of female-biased, male-biased and unbiased genes in floral buds of dioecious *Trichosanthes pilosa* using 'free-ratio' (A) and 'two-ratio' (B) branch model. Significant differences are represented by * in Wilcoxon rank sum tests (***$P < 0.0005$).

Supplementary Figure S5. Venn diagrams of female-biased genes under positive selection in floral buds. Overlaps of female-biased genes were detected to be under positive selection using aBSREL, BUSTED, CodeML and RELAX.

Supplementary Figure S6. Venn diagrams of unbiased genes under positive selection in floral buds. Overlaps of unbiased genes were identified to be under positive selection using aBSREL, BUSTED, CodeML and RELAX.

Supplementary Figure S7. Scatterplots of KEGG pathway of sex-biased genes in female (A) and male (B) floral buds of the dioecious *Trichosanthes pilosa*. The y axis represents the pathway name, and the x axis represents the ratio of genes corresponding to the pathways.

Supplementary Figure S8. The overlap between male-biased genes with faster evolutionary rates and tissue-biased genes in floral buds. M1BGs indicate male-biased genes with faster evolutionary rates in male floral buds (M1-biased genes). M1TGs indicate tissue-biased genes in male floral buds (M1-tissue-biased genes). 343 M1BGs overlapped with 1755 M1TGs (A). 27 out of 343 M1BGs&M1TGs overlapped with M1BGs_98 (B). 27 out of 343 M1BGs&M1TGs overlapped with M1BGs_18 (C).

Supplementary file 2. Supplementary Tables S1 to S14.

Supplementary Table S1. Overview of sequencing reads from 12 samples of male and female plants in *Trichosanthes pilosa*.

Supplementary Table S2. Numbers of unigenes annotated in public databases.

Supplementary Table S3. The mapping rate of reads for each sample in floral buds and flowers at anthesis of *Trichosanthes pilosa*.

Supplementary Table S4. d_N, d_S and ω values of each female-biased, male-biased, unbiased orthologous genes of floral buds and flowers at anthesis for each species using 'two-ratio' branch model of CodeML in PAML. Two dioecious species *Trichosanthes pilosa* and *T. kirilowii* represent the foreground and two monoecious species *T. anguina* and *Luffa cylindrica* represent the background.

707 Supplementary Table S5. d_N, d_S and ω values of each female-biased, male-biased,
708 unbiased orthologous genes of floral buds and flowers at anthesis for each species
709 using 'free-ratio' branch model of CodeML in PAML.
710 Supplementary Table S6. Genes under positive selection identified by branch-site
711 model of CodeML in PAML and function in NR, KEGG, Swissport and GO
712 databases for male-biased orthologous genes in floral buds. Two dioecious
713 species *Trichosanthes pilosa* and *T. kirilowii* represent the foreground and two
714 monoecious species, *T. anguina* and *Luffa cylindrica* represent the background.
715 Supplementary Table S7. Genes under episodic positive selection tested by
716 aBSREL model in HyPhy and functions in NR, KEGG, Swissport and GO
717 databases for male-biased orthologous genes in floral buds. The dioecious species
718 *Trichosanthes pilosa* represents the foreground and other species represent the
719 background.
720 Supplementary Table S8. Genes under episodic positive selection found by
721 BUSTED model in HyPhy and functions in NR, KEGG, Swissport and GO
722 databases for male-biased orthologous genes in floral buds. The dioecious species
723 *Trichosanthes pilosa* represents the foreground (unconstrained branch) and other
724 species represent the background (constrained branch).
725 Supplementary Table S9. Genes under relaxed selection detected by RELAX
726 model in HyPhy and functions in NR, KEGG, Swissport and GO databases for
727 male-biased orthologous genes in floral buds. The dioecious species
728 *Trichosanthes pilosa* represents the foreground (test) and other species represent

729 the background (reference).

730 Supplementary Table S10. Genes under intensified positive selection identified by
731 RELAX model in HyPhy and functions in NR, KEGG, Swissport and GO
732 databases for male-biased orthologous genes in floral buds. The dioecious species
733 *Trichosanthes pilosa* represents the foreground (test) and other species represent
734 the background (reference).

735 Supplementary Table S11. KEGG pathway enrichment analysis of female-biased
736 and male-biased genes in floral buds of the dioecious *Trichosanthes pilosa*.

737 Supplementary Table S12. Functions and references associated with abiotic stress
738 and immune responses, organ developments of male-biased genes under
739 significant positive selection ($P < 0.05$) in floral buds.

740 Supplementary Table S13. Functions and references associated with abiotic stress
741 and immune responses, organ developments of male-biased genes under
742 significant relaxed selection ($P < 0.05$) in floral buds.

743 Supplementary Table S14. The expressions and functions of some male-biased
744 genes associated with senescence, raceme inflorescence development and early
745 flowering in floral buds.

746 **Data Availability**

747 All RNA-Sequencing clean reads have been deposited in the databases of the
748 National Center for Biotechnology Information (NCBI) under BioProject ID
749 PRJNA899312. The reference transcriptome, orthology data, and alignments have

been uploaded to ResearchGate (www.researchgate.net/publication/373194650_Trichosanthes_pilosa_datasets).

References

Abascal F, Zardoya R, Telford MJ. 2010. TranslatorX: multiple alignment of nucleotide sequences guided by amino acid translations. *Nucleic Acids Research* **38**: W7-13.

Álvarez-Carretero S, Kapli P, Yang Z. 2023. Beginner's guide on the use of PAML to detect positive selection. *Molecular Biology and Evolution* **40**: msad041.

Arunkumar R, Josephs EB, Williamson RJ, Wright SI. 2013. Pollen-specific, but not sperm-specific, genes show stronger purifying selection and higher rates of positive selection than sporophytic genes in *Capsella grandiflora*. *Molecular Biology and Evolution* **30**: 2475-2486.

Assis R, Zhou Q, Bachtrog D. 2012. Sex-biased transcriptome evolution in *Drosophila*. *Genome Biology and Evolution* **4**: 1189-1200.

Barrett SCH, Hough J. 2013. Sexual dimorphism in flowering plants. *Journal of Experimental Botany* **64**: 67-82.

Beaudry FEG, Rifkin JL, Barrett SCH, Wright SI. 2020. Evolutionary genomics of plant gametophytic selection. *Plant Communications* **1**: 100115.

Bogamuwa SP, Jang JC. 2014. Tandem CCCH zinc finger proteins in plant growth, development and stress response. *Plant and Cell Physiology* **55**: 1367-1375.

Bolger AM, Lohse M, Usadel B. 2014. Trimmomatic: a flexible trimmer for Illumina

771 sequence data. *Bioinformatics* **30**: 2114-2120.

772 **Boualem A**, Troadec C, Camps C, Lemhemdi A, Morin H, Sari M-A, Fraenkel-
773 Zagouri R, Kovalski I, Dogimont C, Perl-Treves R, Bendahmane A. 2015. A
774 cucurbit androecy gene reveals how unisexual flowers develop and dioecy
775 emerges. *Science* **350**: 688-691.

776 **Cai ZY**, Yang CC, Liao J, Song HF, Zhang S. 2021. Sex-biased genes and metabolites
777 explain morphologically sexual dimorphism and reproductive costs in *Salix*
778 *paraplesia* catkins. *Horticulture Research* **8**: 125.

779 **Catalan A**, Macias-Munoz A, Briscoe AD. 2018. Evolution of sex-biased gene
780 expression and dosage compensation in the eye and brain of *Heliconius*
781 *Butterflies*. *Molecular Biology and Evolution* **35**: 2343-2343.

782 **Charlesworth B**, Campos JL, Jackson BC. 2018. Faster-X evolution: theory and
783 evidence from *Drosophila*. *Molecular Ecology* **27**: 3753-3771.

784 **Charlesworth D**. 2018. Does sexual dimorphism in plants promote sex chromosome
785 evolution? *Environmental and Experimental Botany* **146**: 5-12.

786 **Chen F**, Hu Y, Vannozzi A, Wu K, Cai H, Qin Y, Mullis A, Lin Z, Zhang L. 2017. The
787 WRKY transcription factor family in model plants and crops. *Critical Reviews in*
788 *Plant Sciences* **36**: 311-335.

789 **Conesa A**, Gotz S, Garcia-Gomez JM, Terol J, Talon M, Robles M. 2005. Blast2GO:
790 a universal tool for annotation, visualization and analysis in functional
791 genomics research. *Bioinformatics* **21**: 3674-3676.

792 **Congrains C**, Campanini EB, Torres FR, Rezende VB, Nakamura AM, de Oliveira JL,

Lima ALA, Chahad-Ehlers S, Sobrinho IS, de Brito RA. 2018. Evidence of adaptive evolution and relaxed constraints in sex-biased genes of South American and West Indies fruit flies (Diptera: Tephritidae). *Genome Biology and Evolution* **10**: 380-395.

Cossard GG, Godfroy O, Nehr Z, Cruaud C, Cock JM, Lipinska AP, Coelho SM. 2022. Selection drives convergent gene expression changes during transitions to co-sexuality in haploid sexual systems. *Nature Ecology and Evolution* **6**: 579-589.

Cossard GG, Toups MA, Pannell JR. 2019. Sexual dimorphism and rapid turnover in gene expression in pre-reproductive seedlings of a dioecious herb. *Annals of Botany* **123**: 1119-1131.

Cui YW, Lu XT, Gou XP. 2022. Receptor-like protein kinases in plant reproduction: current understanding and future perspectives. *Plant Communications* **3**: 100273.

Dapper AL, Wade MJ. 2020. Relaxed selection and the rapid evolution of reproductive genes. *Trends in Genetics* **36**: 640-649.

Darolti I, Fong LJM, Sandkam BA, Metzger DCH, Mank JE. 2023. Sex chromosome heteromorphism and the Fast-X effect in poeciliids. *Molecular ecology* **32**: 4599-4609.

Darolti I, Mank JE. 2023. Sex-biased gene expression at single-cell resolution: cause and consequence of sexual dimorphism. *Evolution Letters* **7**: 148-156.

Darolti I, Wright AE, Pucholt P, Berlin S, Mank JE. 2018. Slow evolution of sex-

815 biased genes in the reproductive tissue of the dioecious plant *Salix viminalis*.
816 *Molecular ecology* **27**: 694-708.
817 **Davidson NM**, Oshlack A. 2014. Corset: enabling differential gene expression
818 analysis for *de novo* assembled transcriptomes. *Genome Biology* **15**: 410.
819 **Dawson TE**, Geber MA. 1999. Sexual dimorphism in physiology and morphology.
820 In: Geber MA, Dawson TE, Delph LF (Eds). *Gender and Sexual Dimorphism*
821 *in Flowering Plants*. Berlin, Heidelberg: Springer. p. 175-215.
822 **de Boer HJ**, Schaefer H, Thulin M, Renner SS. 2012. Evolution and loss of long-
823 fringed petals: a case study using a dated phylogeny of the snake gourds,
824 *Trichosanthes* (Cucurbitaceae). *BMC Ecology and Evolution* **12**: 108.
825 **de Boer HJ**, Steffen K, Cooper WE. 2015. Sunda to Sahul dispersals in *Trichosanthes*
826 (Cucurbitaceae): a dated phylogeny reveals five independent dispersal events
827 to Australasia. *Journal of Biogeography* **42**: 519-531.
828 **Delph LF**. 1999. Sexual dimorphism in life history. In: Geber MA, Dawson TE,
829 Delph LF (Eds). *Gender and Sexual Dimorphism in Flowering Plants*. Berlin,
830 Heidelberg: Springer. p. 149-173.
831 **Delph LF**, Herlihy CR. 2012. Sexual, fecundity, and viability selection on flower size
832 and number in a sexually dimorphic plant. *Evolution* **66**: 1154-1166.
833 **Djordjevic J**, Dumas Z, Robinson-Rechavi M, Schwander T, Parker DJ. 2022.
834 Dynamics of sex-biased gene expression during development in the stick
835 insect *Timema californicum*. *Heredity* **129**: 113-122.
836 **Ellegren H**, Parsch J. 2007. The evolution of sex-biased genes and sex-biased gene

expression. *Nature Reviews Genetics* **8**: 689-698.

Emms DM, Kelly S. 2019. OrthoFinder: phylogenetic orthology inference for comparative genomics. *Genome Biology* **20**: 238.

Fellows I. 2012. Deducer: a data analysis GUI for R. *Journal of Statistical Software* **49**: 1-15.

Forrest JRK. 2014. Plant size, sexual selection, and the evolution of protandry in dioecious plants. *American Naturalist* **184**: 338-351.

Frumkin I, Lajoie MJ, Gregg CJ, Hornung G, Church GM, Pilpel Y. 2018. Codon usage of highly expressed genes affects proteome-wide translation efficiency. *Proceedings of the National Academy of Sciences* **115**: E4940-E4949.

Gershoni M, Pietrokovski S. 2014. Reduced selection and accumulation of deleterious mutations in genes exclusively expressed in men. *Nature Communications* **5**: 4438.

Gossmann TI, Schmid MW, Grossniklaus U, Schmid KJ. 2014. Selection-driven evolution of sex-biased genes is consistent with sexual selection in *Arabidopsis thaliana*. *Molecular Biology and Evolution* **31**: 574-583.

Gossmann TI, Saleh D, Schmid MW, Spence MA, Schmid KJ. 2016. Transcriptomes of plant gametophytes have a higher proportion of rapidly evolving and young genes than sporophytes. *Molecular Biology and Evolution* **33**: 1669-1678.

Grath S, Parsch J. 2016. Sex-biased gene expression. *Annual Review of Genetics* **50**: 29-44.

Guo J, Xu W, Hu Y, Huang J, Zhao Y, Zhang L, Huang CH, Ma H. 2020.

Phylotranscriptomics in Cucurbitaceae reveal multiple whole-genome duplications and key morphological and molecular innovations. *Molecular Plant* **13**: 1117-1133.

Gutierrez-Valencia J, Fracassetti M, Horvath R, Laenen B, Desamore A, Drouzas AD, Friberg M, Kolar F, Slotte T. 2022. Genomic signatures of sexual selection on pollen-expressed genes in *Arabis alpina*. *Molecular Biology and Evolution* **39**: msab349.

Haas BJ, Papanicolaou A, Yassour M, Grabherr M, Blood PD, Bowden J, Couger MB, Eccles D, Li B, Lieber M, et al. 2013. *De novo* transcript sequence reconstruction from RNA-seq using the Trinity platform for reference generation and analysis. *Nature Protocols* **8**: 1494-1512.

Hajdu A, Adam E, Sheerin DJ, Dobos O, Bernula P, Hiltbrunner A, Kozma-Bognar L, Nagy F. 2015. High-level expression and phosphorylation of phytochrome B modulates flowering time in *Arabidopsis*. *Plant Journal* **83**: 794-805.

Hambuch TM, Parsch J. 2005. Patterns of synonymous codon usage in *Drosophila melanogaster* genes with sex-biased expression. *Genetics* **170**: 1691-1700.

Harkess A, Mercati F, Shan HY, Sunseri F, Falavigna A, Leebens-Mack J. 2015. Sex-biased gene expression in dioecious garden asparagus (*Asparagus officinalis*). *New Phytologist* **207**: 883-892.

Harrison MC, Mallon EB, Twell D, Hammond RL. 2019. Deleterious mutation accumulation in *Arabidopsis thaliana* pollen genes: a role for a recent relaxation of selection. *Genome Biology and Evolution* **11**: 1939-1951.

881 **Harrison PW**, Wright AE, Zimmer F, Dean R, Montgomery SH, Pointer MA, Mank
882 JE. 2015. Sexual selection drives evolution and rapid turnover of male gene
883 expression. *Proceedings of the National Academy of Sciences of the United*
884 *States of America* **112**: 4393-4398.
885 **Hatchett WJ**, Jueterbock AO, Kopp M, Coyer JA, Coelho SM, Hoarau G, Lipinska AP.
886 2023. Evolutionary dynamics of sex-biased gene expression in a young XY system:
887 Insights from the brown alga genus *Fucus*. *New Phytologist* **238**: 422-437.
888 **Hou JJ**, Fan WW, Ma RR, Li B, Yuan ZH, Huang WX, Wu YY, Hu Q, Lin CJ, Zhao
889 XQ, et al. 2022. *MALE STERILITY 3* encodes a plant homeodomain-finger
890 protein for male fertility in soybean. *Journal of Integrative Plant Biology* **64**:
891 1076-1086.
892 **Hough J**, Hollister JD, Wang W, Barrett SCH, Wright SI. 2014. Genetic degeneration
893 of old and young Y chromosomes in the flowering plant *Rumex hastatulus*.
894 *Proceedings of the National Academy of Sciences* **111**: 7713-7718.
895 **Hsu S-K**, Jakšić AM, Nolte V, Lirakis M, Kofler R, Barghi N, Versace E, Schlötterer
896 C. 2020. Rapid sex-specific adaptation to high temperature in *Drosophila*.
897 *Elife* **9**: e53237.
898 **Hu XQ**, Liao ZY, Zhang B, Yue JJ, Wang Z, Jie X, Liu J. 2020. Transcriptome
899 sequencing and screening of genes related to sex determination of
900 *Trichosanthes kirilowii* Maxim. *PLoS One* **15**: e0239230.
901 **Hudson M**, Smith H. 1998. The phytochrome B encoded by the *HLG* locus of
902 *Nicotiana plumbaginifolia* is required for detection of photoperiod: *hlg*

903 mutants show altered regulation of flowering and circadian movement. *Plant*
904 *Journal* **15**: 281-287.
905 **Immler S**. 2019. Haploid selection in "diploid" organisms. *Annual Review of Ecology,*
906 *Evolution, and Systematics* **50**: 219-236.
907 **Jones P**, Binns D, Chang HY, Fraser M, Li W, McAnulla C, McWilliam H, Maslen J,
908 Mitchell A, Nuka G, et al. 2014. InterProScan 5: genome-scale protein
909 function classification. *Bioinformatics* **30**: 1236-1240.
910 **Khodursky S**, Svetec N, Durkin SM, Zhao L. 2020. The evolution of sex-biased gene
911 expression in the *Drosophila* brain. *Genome Research* **30**: 874-884.
912 **Lahti DC**, Johnson NA, Ajie BC, Otto SP, Hendry AP, Blumstein DT, Coss RG,
913 Donohue K, Foster SA. 2009. Relaxed selection in the wild. *Trends in Ecology*
914 *and Evolution* **24**: 487-496.
915 **Langmead B**, Salzberg SL. 2012. Fast gapped-read alignment with Bowtie 2. *Nature*
916 *Methods* **9**: 357-359.
917 **Li B**, Dewey CN. 2011. RSEM: accurate transcript quantification from RNA-Seq data
918 with or without a reference genome. *BMC Bioinformatics* **12**: 323.
919 **Li SH**, Yan H, Mei WM, Tse YC, Wang H. 2020. Boosting autophagy in sexual
920 reproduction: a plant perspective. *New Phytologist* **226**: 679-689.
921 **Lichilin** N, El Taher A, Bohne A. 2021. Sex-biased gene expression and recent sex
922 chromosome turnover. *Philosophical Transactions of the Royal Society B:*
923 *Biological Sciences* **376**: 20200107.
924 **Lipinska A**, Cormier A, Luthringer R, Peters AF, Corre E, Gachon CM, Cock JM,

925 Coelho SM. 2015. Sexual dimorphism and the evolution of sex-biased gene
926 expression in the brown alga *ectocarpus*. *Molecular Biology and Evolution* **32**:
927 1581-1597.
928 **Liu ZH**, Tavares R, Forsythe ES, Andre F, Lugan R, Jonasson G, Boutet-Mercey S,
929 Tohge T, Beilstein MA, et al. 2016. Evolutionary interplay between sister
930 cytochrome P450 genes shapes plasticity in plant metabolism. *Nature*
931 *Communications* **7**: 13026.
932 **Liu Y**, Bassham DC. 2012. Autophagy: pathways for self-eating in plant cells. *Annual*
933 *Review of Plant Biology* **63**: 215-237.
934 **Love MI**, Huber W, Anders S. 2014. Moderated estimation of fold change and
935 dispersion for RNA-seq data with DESeq2. *Genome Biology* **15**: 550.
936 **Lynch M**, Conery JS. 2000. The evolutionary fate and consequences of duplicate genes.
937 *Science* **290**: 1151-1155.
938 **Lynch M**, Katju V. 2004. The altered evolutionary trajectories of gene duplicates.
939 *Trends in Genetics* **20**: 544-549.
940 **Ma LL**, Wang Q, Mu JL, Fu AZ, Wen CL, Zhao XY, Gao LP, Li J, Shi K, Wang YX,
941 et al. 2020. The genome and transcriptome analysis of snake gourd provide
942 insights into its evolution and fruit development and ripening. *Horticulture*
943 *Research* **7**: 199.
944 **Ma WJ**, Pannell JR. 2016. Sex determination: separate sexes are a double turnoff in
945 melons. *Current Biology* **26**: R171-R174.
946 **Mank JE**. 2009. Sex chromosomes and the evolution of sexual dimorphism: lessons

947 from the genome. *American Naturalist* **173**: 141-150.

948 **Mank JE**. 2017. The transcriptional architecture of phenotypic dimorphism. *Nature*
949 *Ecology and Evolution* **1**: 6.

950 **Mank JE.** 2023. Sex-specific morphs: the genetics and evolution of intra-sexual
951 variation. *Nature Reviews Genetics* **24**: 44-52.

952 **Mank JE**, Hultin-Rosenberg L, Axelsson E, Ellegren H. 2007. Rapid evolution of
953 female-biased, but not male-biased, genes expressed in the avian brain.
954 *Molecular Biology and Evolution* **24**: 2698-2706.

955 **Mao XZ**, Cai T, Olyarchuk JG, Wei LP. 2005. Automated genome annotation and
956 pathway identification using the KEGG Orthology (KO) as a controlled
957 vocabulary. *Bioinformatics* **21**: 3787-3793.

958 **Marinić M**, Lynch VJ. 2020. Relaxed constraint and functional divergence of the
959 progesterone receptor (*PGR*) in the human stem-lineage. *PLOS Genetics* **16**:
960 e1008666.

961 **Meisel RP.** 2011. Towards a more nuanced understanding of the relationship between
962 sex-biased gene expression and rates of protein-coding sequence evolution.
963 *Molecular Biology and Evolution* **28**: 1893-1900.

964 **Meisel RP**, Connallon T. 2013. The faster-X effect: integrating theory and data.
965 *Trends in Genetics* **29**: 537-544.

966 **Ming R**, Bendahmane A, Renner SS. 2011. Sex chromosomes in land plants. *Annual*
967 *Review of Plant Biology* **62**: 485-514.

968 **Moore JC**, Pannell JR. 2011. Sexual selection in plants. *Current Biology* **21**: R176-

969 R182.

970 **Moriya Y**, Itoh M, Okuda S, Yoshizawa AC, Kanehisa M. 2007. KAAS: an automatic
971 genome annotation and pathway reconstruction server. *Nucleic Acids Research*
972 **35**: W182-185.

973 **Moyle LC**, Wu M, Gibson MJS. 2021. Reproductive proteins evolve faster than non-
974 reproductive proteins among *Solanum* species. *Frontiers in Plant Science* **12**:
975 635990.

976 **Murat F**, Mbengue N, Winge SB, Trefzer T, Leushkin E, Sepp M, Cardoso-Moreira
977 M, Schmidt J, Schneider C, Mößinger K, et al. 2023. The molecular evolution
978 of spermatogenesis across mammals. *Nature* **613**: 308-316.

979 **Murrell B**, Weaver S, Smith MD, Wertheim JO, Murrell S, Aylward A, Eren K,
980 Pollner T, Martin DP, Smith DM, et al. 2015. Gene-wide identification of
981 episodic selection. *Molecular Biology and Evolution* **32**: 1365-1371.

982 **Muschietti JP**, Wengier DL. 2018. How many receptor-like kinases are required to
983 operate a pollen tube. *Current Opinion in Plant Biology* **41**: 73-82.

984 **Muyle A.** 2019. How different is the evolution of sex-biased gene expression between
985 plants and animals? A commentary on: 'Sexual dimorphism and rapid turnover
986 in gene expression in prereproductive seedlings of a dioecious herb'. *Annals of*
987 *Botany* **123**: iv-v.

988 **Naqvi S**, Godfrey AK, Hughes JF, Goodheart ML, Mitchell RN, Page DC. 2019.
989 Conservation, acquisition, and functional impact of sex-biased gene
990 expression in mammals. *Science* **365**: eaaw7317.

Palmer DH, Rogers TF, Dean R, Wright AE. 2019. How to identify sex chromosomes and their turnover. *Molecular ecology* **28**: 4709-4724.

Papa F, Windbichler N, Waterhouse RM, Cagnetti A, D'Amato R, Persampieri T, Lawniczak MKN, Nolan T, Papathanos PA. 2017. Rapid evolution of female-biased genes among four species of *Anopheles* malaria mosquitoes. *Genome Research* **27**: 1536-1548.

Parsch J, Ellegren H. 2013. The evolutionary causes and consequences of sex-biased gene expression. *Nature Reviews Genetics* **14**: 83-87.

Parvathy ST, Udayasuriyan V, Bhadana V. 2022. Codon usage bias. *Molecular Biology Reports* **49**: 539-565.

Pond SLK, Poon AFY, Velazquez R, Weaver S, Hepler NL, Murrell B, Shank SD, Magalis BR, Bouvier D, Nekrutenko A, et al. 2020. HyPhy 2.5–a customizable platform for evolutionary hypothesis testing using phylogenies. *Molecular Biology and Evolution* **37**: 295-299.

Pröschel M, Zhang Z, Parsch J. 2006. Widespread adaptive evolution of *Drosophila* genes with sex-biased expression. *Genetics* **174**: 893-900.

Ren J, Wu Y, Zhu Z, Chen R, Zhang L. 2022. Biosynthesis and regulation of diterpenoids in medicinal plants. *Chinese Journal of Natural Medicines* **20**: 761-772.

Renner SS. 2014. The relative and absolute frequencies of angiosperm sexual systems: dioecy, monoecy, gynodioecy, and an updated online database. *American Journal of Botany* **101**: 1588-1596.

1013 **Rowe L**, Chenoweth SF, Agrawal AF. 2018. The genomics of sexual conflict. *American*
1014 *Naturalist* **192**: 274-286.
1015 **Sanderson BJ**, Wang L, Tiffin P, Wu ZQ, Olson MS. 2019. Sex-biased gene
1016 expression in flowers, but not leaves, reveals secondary sexual dimorphism in
1017 *Populus balsamifera*. *New Phytologist* **221**: 527-539.
1018 **Sandler G**, Beaudry FEG, Barrett SCH, Wright SI. 2018. The effects of haploid
1019 selection on Y chromosome evolution in two closely related dioecious plants.
1020 *Evolution Letters* **2**: 368-377.
1021 **Schaefer H**, Renner SS. 2010. A three-genome phylogeny of *Momordica*
1022 (Cucurbitaceae) suggests seven returns from dioecy to monoecy and recent
1023 long-distance dispersal to Asia. *Molecular Phylogenetics and Evolution* **54**:
1024 553-560.
1025 **Schaefer H**, Renner SS. 2011. Phylogenetic relationships in the order Cucurbitales
1026 and a new classification of the gourd family (Cucurbitaceae). *Taxon* **60**: 122-
1027 138.
1028 **Scharf KD**, Berberich T, Ebersberger I, Nover L. 2012. The plant heat stress
1029 transcription factor (Hsf) family: structure, function and evolution. *Biochimica*
1030 *Et Biophysica Acta-Gene Regulatory Mechanisms* **1819**: 104-119.
1031 **Scharmann M**, Rebelo AG, Pannell JR. 2021. High rates of evolution preceded shifts
1032 to sex-biased gene expression in *Leucadendron*, the most sexually dimorphic
1033 angiosperms. *eLife* **10**: e67485.
1034 **Schrader L**, Pan H, Bollazzi M, Schiott M, Larabee FJ, Bi X, Deng Y, Zhang G,

1035 Boomsma JJ, Rabeling C. 2021. Relaxed selection underlies genome erosion
1036 in socially parasitic ant species. *Nature Communications* **12**: 2918.
1037 **Seppey M**, Manni M, Zdobnov EM. 2019. BUSCO: Assessing genome assembly and
1038 annotation completeness. *Methods in Molecular Biology* **1962**: 227-245.
1039 **Shiryev SA**, Papadopoulos JS, Schaffer AA, Agarwala R. 2007. Improved BLAST
1040 searches using longer words for protein seeding. *Bioinformatics* **23**: 2949-
1041 2951.
1042 **Singh A**, Agrawal AF. 2023. Two forms of sexual dimorphism in gene expression in
1043 *Drosophila melanogaster*: their coincidence and evolutionary genetics.
1044 *Molecular Biology and Evolution* **40**: msad091.
1045 **Skogsmyr I**, Lankinen A. 2002. Sexual selection: an evolutionary force in plants.
1046 *Biological Reviews* **77**: 537-562.
1047 **Smith MD**, Wertheim JO, Weaver S, Murrell B, Scheffler K, Pond SLK. 2015. Less is
1048 more: an adaptive branch-site random effects model for efficient detection of
1049 episodic diversifying selection. *Molecular Biology and Evolution* **32**: 1342-
1050 1353.
1051 **Stephenson AG**, Bertin RI. 1983. Male competition, female choice, and sexual
1052 selection in plants. In: Real L (Eds). *Pollination Biology*. New York, NY,
1053 USA: Academic Press. p.109-151.
1054 **Teo ZWN**, Song SY, Wang YQ, Liu J, Yu H. 2014. New insights into the regulation of
1055 inflorescence architecture. *Trends in Plant Science* **19**: 158-165.
1056 **Tosto NM**, Beasley ER, Wong BBM, Mank JE, Flanagan SP. 2023. The roles of sexual

1057 selection and sexual conflict in shaping patterns of genome and transcriptome
1058 variation. *Nature Ecology and Evolution* **7**: 981-993
1059 **Toubiana W**, Armisén D, Dechaud C, Arbore R, Khila A. 2021. Impact of male trait
1060 exaggeration on sex-biased gene expression and genome architecture in a
1061 water strider. *BMC Biology* **19**: 89
1062 **Vaughan MM**, Wang Q, Webster FX, Kiemle D, Hong YJ, Tantillo DJ, Coates RM,
1063 Wray AT, Askew W, O'Donnell C, *et al.* 2013. Formation of the unusual
1064 semivolatile diterpene rhizathalene by the *Arabidopsis* class I terpene synthase
1065 TPS08 in the root stele is involved in defense against belowground herbivory.
1066 *The Plant Cell* **25**: 1108-1125.
1067 **Veltsos P**. 2019. Not all sex-biased genes are the same. *New Phytologist* **221**: 10-11.
1068 **Wertheim JO**, Murrell B, Smith MD, Kosakovsky Pond SL, Scheffler K. 2015.
1069 RELAX: detecting relaxed selection in a phylogenetic framework. *Molecular*
1070 *Biology and Evolution* **32**: 820-832.
1071 **Whittle CA**, Kulkarni A, Extavour CG. 2021. Evolutionary dynamics of sex-biased
1072 genes expressed in cricket brains and gonads. *Journal of Evolutionary Biology*
1073 **34**: 1188-1211.
1074 **Williams JH**, Reese JB. 2019. Evolution of development of pollen performance.
1075 *Current Topics in Developmental Biology* **131**: 299-336.
1076 **Wright AE**, Harrison PW, Zimmer F, Montgomery SH, Pointer MA, Mank JE. 2015.
1077 Variation in promiscuity and sexual selection drives avian rate of Faster-Z
1078 evolution. *Molecular Ecology* **24**: 1218-1235.

1079 **Wright F**. 1990. The effective number of codons used in a gene. *Gene* **87**: 23-29.

1080 **Wu H**, Zhao G, Gong H, Li J, Luo C, He X, Luo S, Zheng X, Liu X, Guo J, et al.
1081 2020. A high-quality sponge gourd (*Luffa cylindrica*) genome. *Horticulture*
1082 *Research* **7**: 128.

1083 **Wu Z**, Raven P, Hong D. 2011. *Flora of China.* Beijing, China: Science Press, and St.
1084 Louis, USA: Missouri Botanical Garden Press.

1085 **Yang Z**. 2007. PAML 4: phylogenetic analysis by maximum likelihood. *Molecular*
1086 *Biology and Evolution* **24**: 1586-1591.

1087 **Yang ZH**, Wong WSW, Nielsen R. 2005. Bayes empirical bayes inference of amino
1088 acid sites under positive selection. *Molecular Biology and Evolution* **22**: 1107-
1089 1118.

1090 **Yue T**, Guo Y, Qi X, Zheng W, Zhang H, Wang B, Liu K, Zhou B, Zeng X,
1091 Ouzhuluobu, He Y, Su B. 2023. Sex-biased regulatory changes in the placenta
1092 of native highlanders contribute to adaptive fetal development. *eLife* **12**:
1093 RP89004

1094 **Zemp N**, Tavares R, Muyle A, Charlesworth D, Marais GA, Widmer A. 2016.
1095 Evolution of sex-biased gene expression in a dioecious plant. *Nature Plants* **2**:
1096 16168.

1097 **Zhang JZ**, Nielsen R, Yang ZH. 2005. Evaluation of an improved branch-site
1098 likelihood method for detecting positive selection at the molecular level.
1099 *Molecular Biology and Evolution* **22**: 2472-2479.

1100 **Zhang MM**, Zhang SQ. 2022. Mitogen-activated protein kinase cascades in plant

signaling. *Journal of Integrative Plant Biology* **64**: 301-341.

Zhang LB, Simmons MP, Kocyan A, Renner SS. 2006. Phylogeny of the Cucurbitales based on DNA sequences of nine loci from three genomes: implications for morphological and sexual system evolution. *Molecular Phylogenetics and Evolution* **39**: 305-322.

Zheng Y, Wu S, Bai Y, Sun HH, Jiao C, Guo SG, Zhao K, Blanca J, Zhang ZH, Huang SW, et al. 2019. Cucurbit Genomics Database (CuGenDB): a central portal for comparative and functional genomics of cucurbit crops. *Nucleic Acids Research* **47**: D1128-D1136.

Zhang Y, Sturgill D, Parisi M, Kumar S, Oliver B. 2007. Constraint and turnover in sex-biased gene expression in the genus *Drosophila*. *Nature* **450**: 233-237.

Zhang YW, Li ZW, Ma B, Hou QC, Wan XY. 2020. Phylogeny and functions of LOB domain proteins in plants. *International Journal of Molecular Sciences* **21**: 2278.

Zhang Z, Hambuch TM, Parsch J. 2004. Molecular evolution of sex-biased genes in *Drosophila*. *Molecular Biology and Evolution* **21**: 2130-2139.

Zhang Z, Parsch J. 2005. Positive correlation between evolutionary rate and recombination rate in *Drosophila* genes with male-biased expression. *Molecular Biology and Evolution* **22**: 1945-1947.

Zhou XM, Zhao P, Sun MX. 2021. Autophagy in sexual plant reproduction: new insights. *Journal of Experimental Botany* **72**: 7658-7667.

Zhou XM, Zhao P, Wang W, Zou J, Cheng TH, Peng XB, Sun MX. 2015. A

comprehensive, genome-wide analysis of autophagy-related genes identified in tobacco suggests a central role of autophagy in plant response to various environmental cues. *DNA Research* **22**: 245-257.

Figure Legends

Fig. 1 Floral buds and flowers at anthesis of females (A, B) and males (C) in *Trichosanthes pilosa.*

Fig. 2 Sex-biased gene expression for floral buds and flowers at anthesis in males and females of *Trichosanthes pilosa.* Volcano plots of average expression between female-biased, male-biased and unbiased genes in floral buds (A) and flowers at anthesis (B). M1 and F1 indicate male and female floral buds; M2 and F2 indicate male and female flowers at anthesis. The value of y coordinate represents $-\log_{10}$(FDR), and the value of x coordinate represents $\log_2$(Fold Change) identified by DESeq2. Heatmap of sex-biased gene expression (C) using hierarchical clustering analysis. Hierarchical gene clustering is based on Euclidean distance with an average of $\log_2$(FPKM) for differentially expressed genes. The color gradient represents from high to low (from red to green) gene expression.

Fig. 3 The overlap between sex-biased and tissue-biased genes in two types of sexes and tissues. Male-biased genes in floral buds (M1BGs) (A) or flowers at anthesis (M2BGs) (B) overlapped with tissue-biased genes in floral buds (M1TGs) and flowers at anthesis (M2TGs). Female-biased genes in floral buds (F1BGs) (C) or flowers at anthesis (F2BGs) (D) overlapped with tissue-biased genes in floral buds

(F1TGs) and flowers at anthesis (F2TGs).

Fig. 4 Violin plots of d_N/d_S values ($0 < \omega < 2$) of female-biased, male-biased and unbiased genes in floral buds and flowers at anthesis of *Trichosanthes pilosa*. White dot indicates the median of d_N/d_S values for sex-biased and unbiased genes. Wilcoxon rank sum tests are used to test for significant differences (***$P < 0.0005$, **$P < 0.005$ and *$P < 0.05$). The distributions of d_N/d_S values for female-biased, male-biased and unbiased genes in floral buds (A) and flowers at anthesis (B) using 'two-ratio' branch model. The distributions of d_N/d_S values for female-biased, male-biased and unbiased genes in floral buds (C) and flowers at anthesis (D) using 'free-ratio' branch model.

Fig. 5 Venn diagrams of male-biased genes detected to be under positive selection using aBSREL, BUSTED, CodeML and RELAX in floral buds.

A
B
C

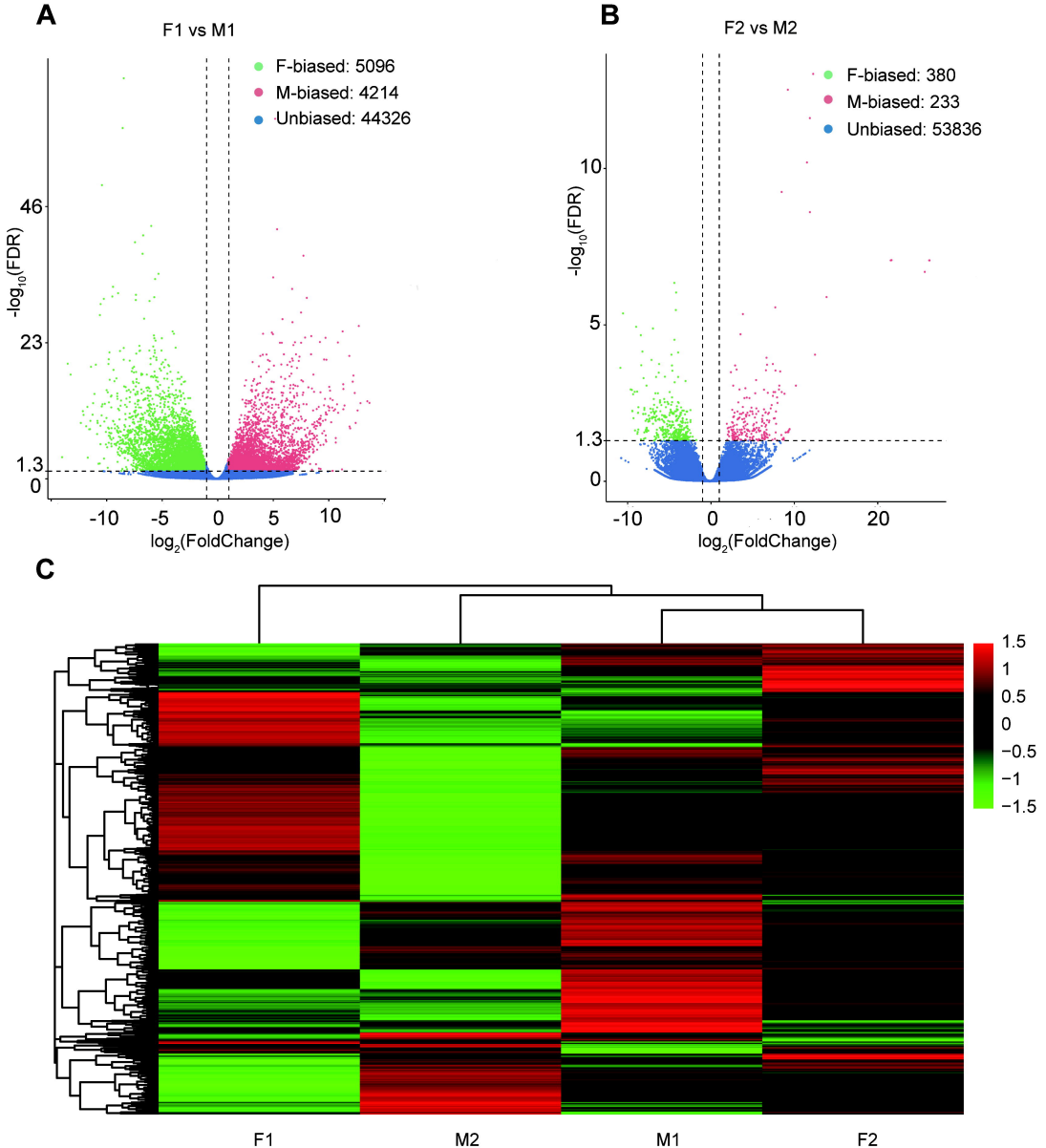
A
F1 vs M1
F-biased: 5096
M-biased: 4214
Unbiased: 44326
-log10(FDR)
46
23
1.3
0
-10
-5
0
5
10
log2(FoldChange)
B
F2 vs M2
F-biased: 380
M-biased: 233
Unbiased: 53836
-log10(FDR)
10
5
1.3
0
-10
0
10
20
log2(FoldChange)
C
1.5
1
0.5
0
−0.5
−1
−1.5
F1
M2
M1
F2

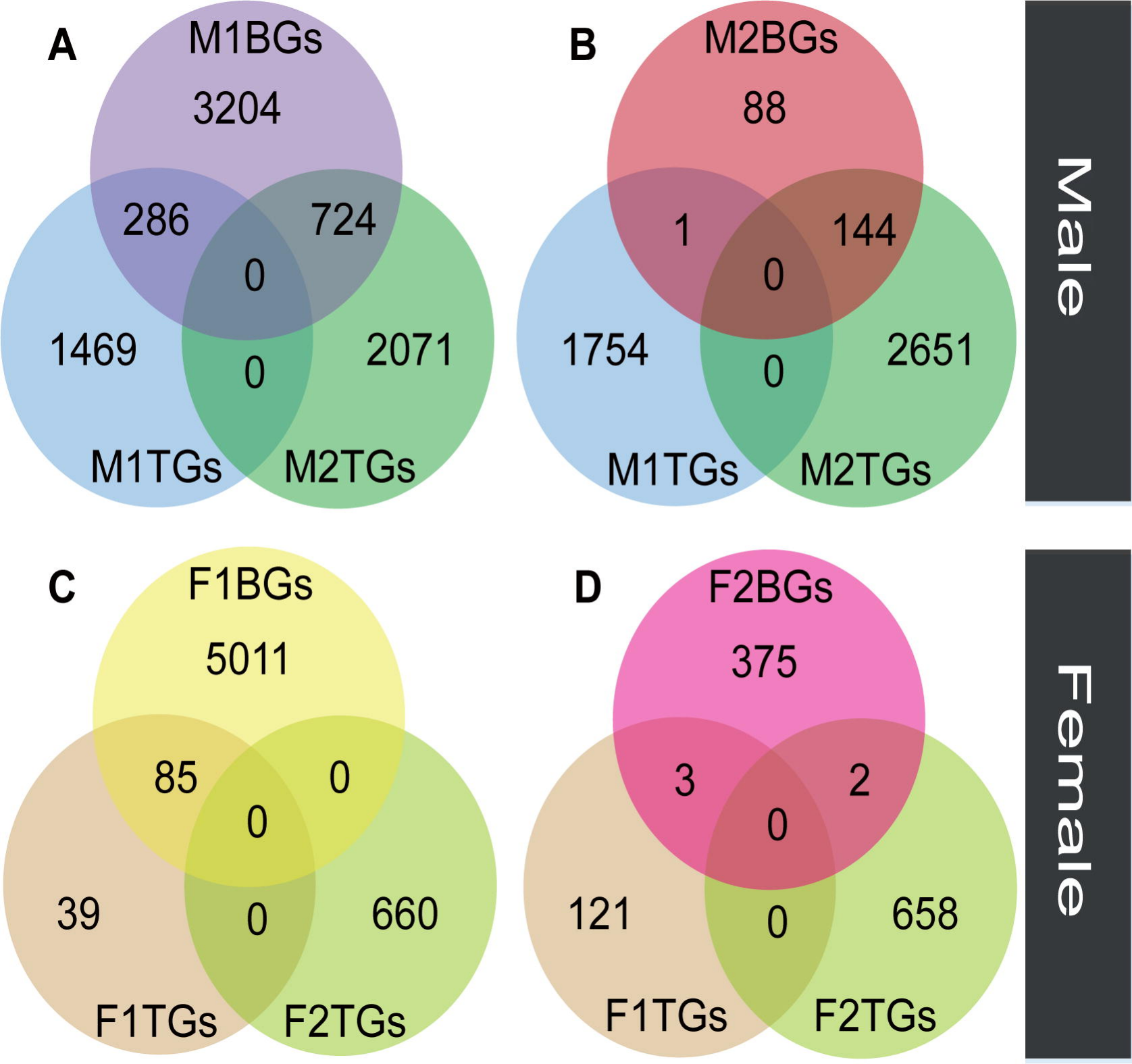
A
M1BGs
3204
286
724
0
1469
0
2071
M1TGs
M2TGs
B
M2BGs
88
1
144
0
1754
0
2651
M1TGs
M2TGs
Male
C
F1BGs
5011
85
0
0
39
0
660
F1TGs
F2TGs
D
F2BGs
375
3
2
0
121
0
658
F1TGs
F2TGs
Female

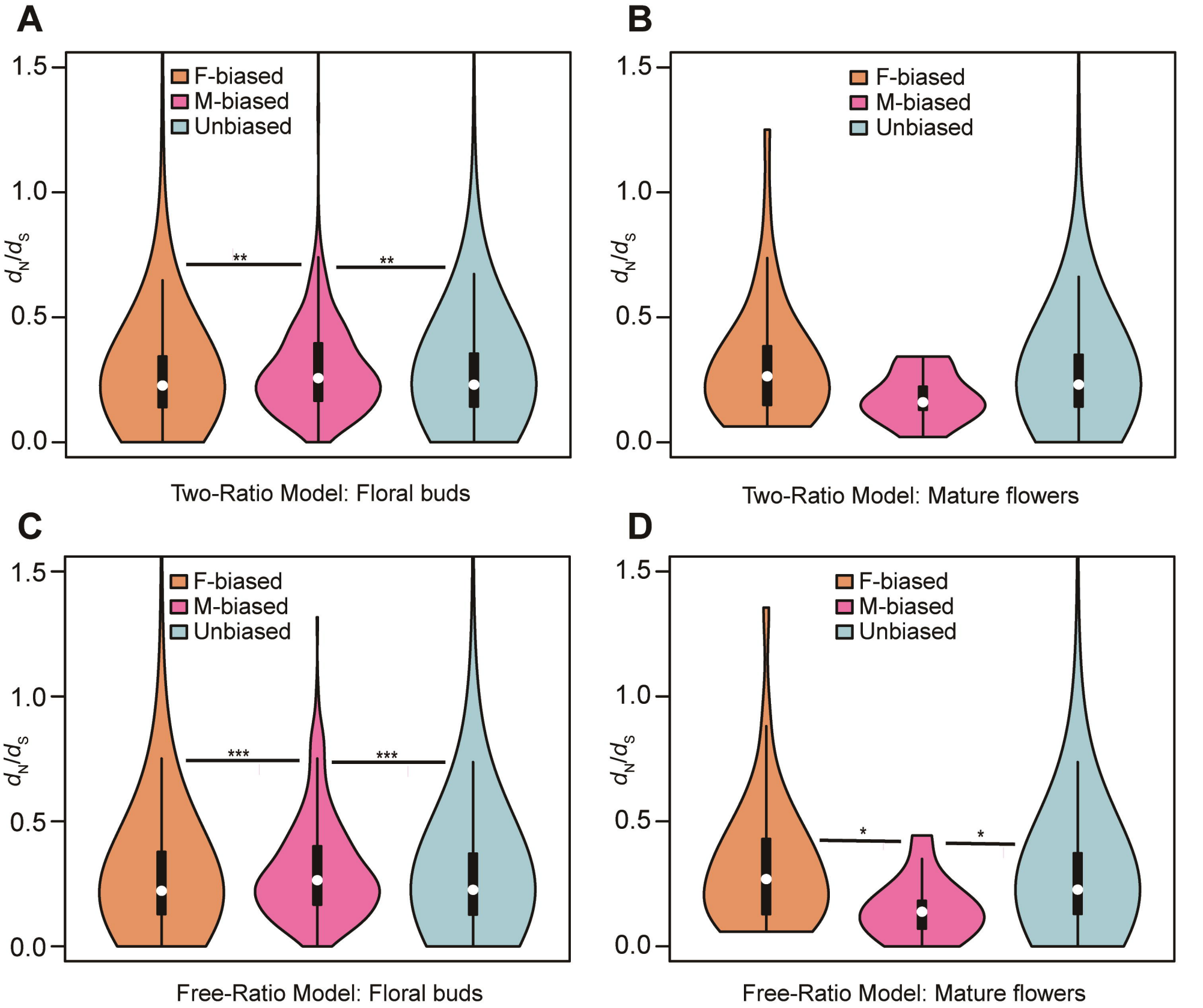
A
B
C
D
F-biased
M-biased
Unbiased
d_N/d_S
1.5
1.0
0.5
0.0
**
***
*
Two-Ratio Model: Floral buds
Two-Ratio Model: Mature flowers
Free-Ratio Model: Floral buds
Free-Ratio Model: Mature flowers

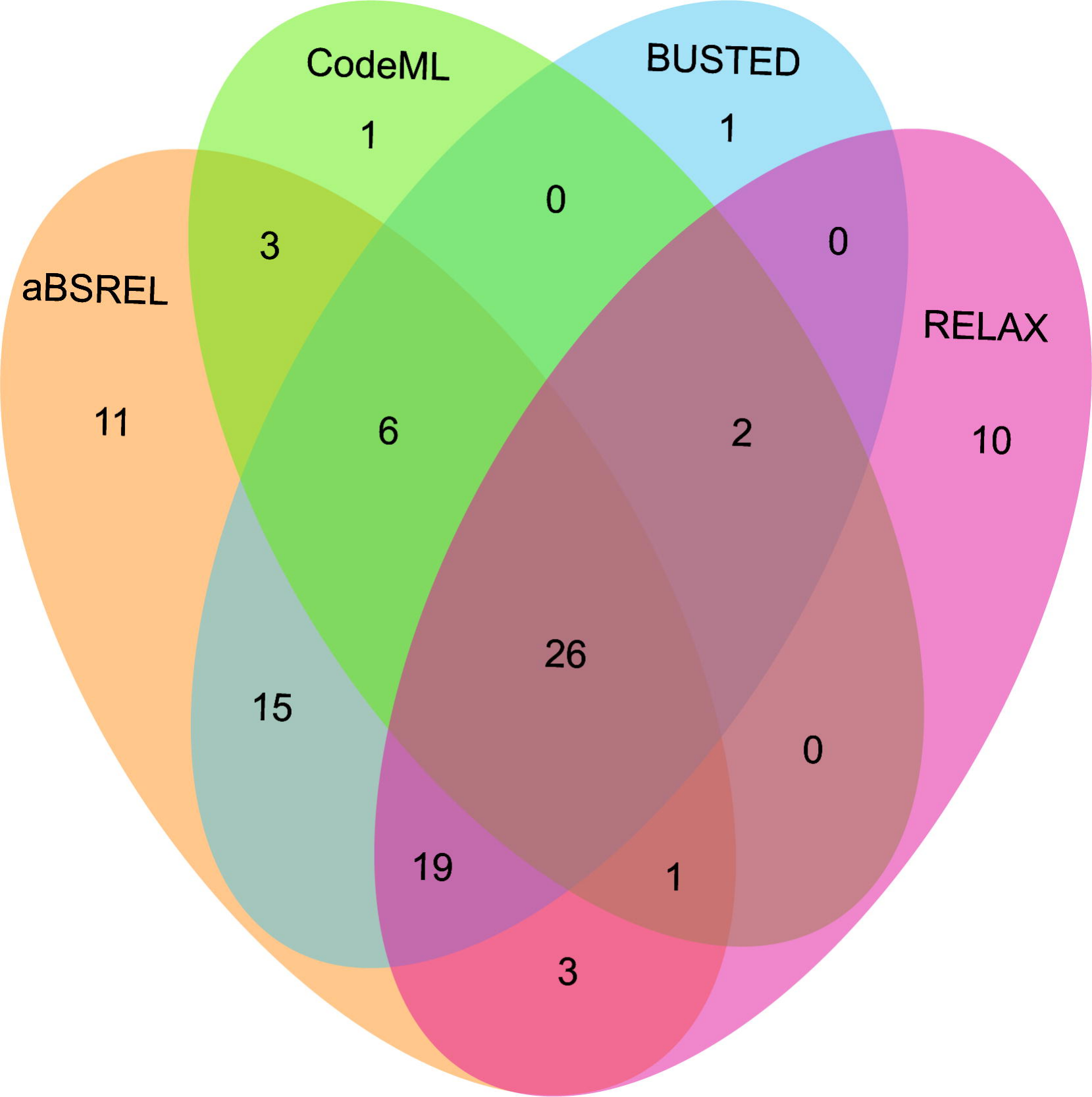
CodeML
BUSTED
aBSREL
RELAX
1
1
0
3
0
11
6
2
10
26
15
0
19
1
3